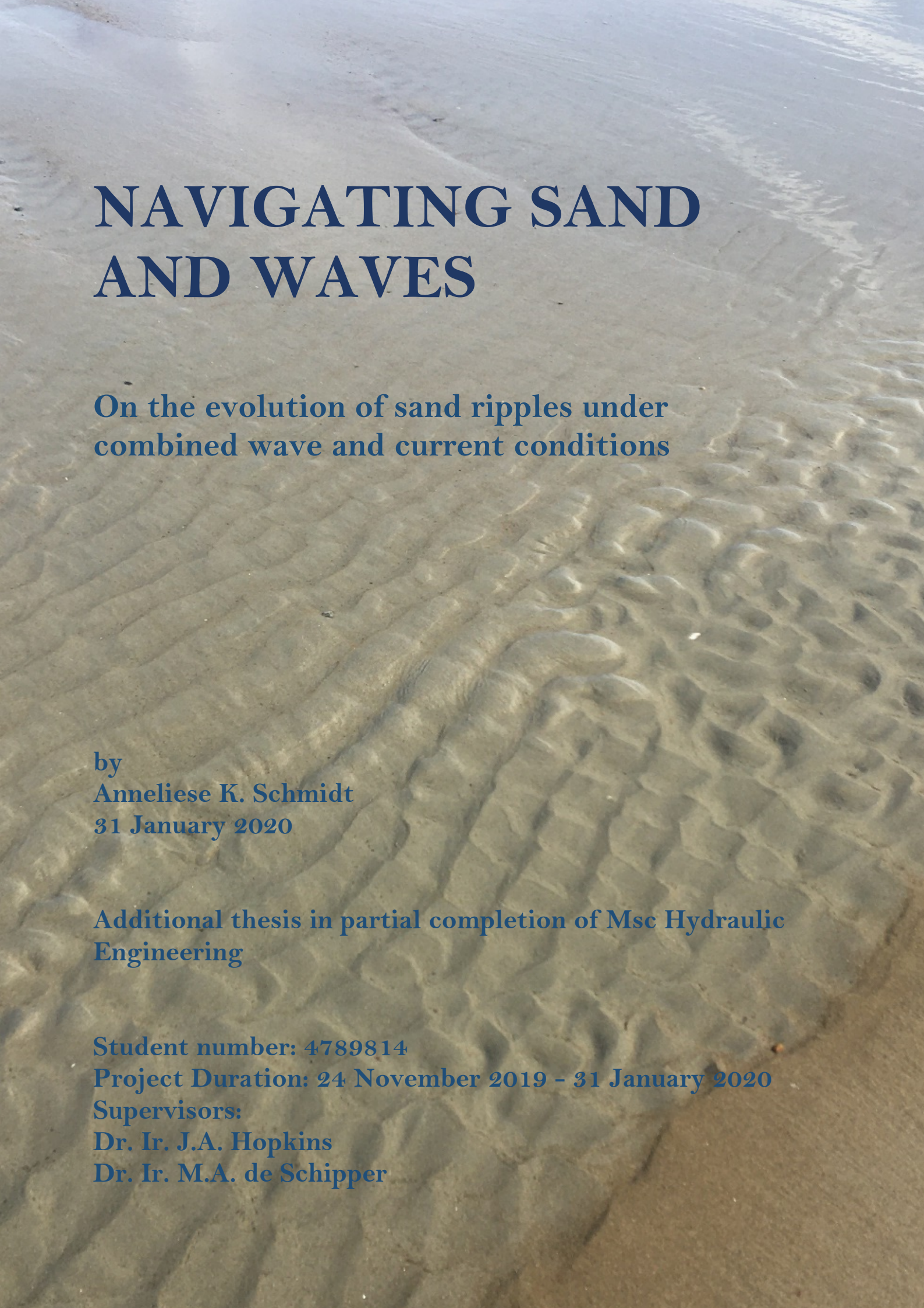

NAVIGATING SAND AND WAVES

On the evolution of sand ripples under combined wave and current conditions

by
Anneliese K. Schmidt
31 January 2020

Additional thesis in partial completion of Msc Hydraulic Engineering

Student number: 4789814
Project Duration: 24 November 2019 - 31 January 2020
Supervisors:
Dr. Ir. J.A. Hopkins
Dr. Ir. M.A. de Schipper

Abstract
Sand ripples are small (10 cm height) bed forms which occur in the nearshore and surf zone under the impact of both waves and currents. They impact the roughness of the bed used in models of this zone, and contribute to sediment transport. Predictions of their geometry are important to properly model roughness, so correlations between the waves and ripples need to be established. In this project, data about the instantaneous bed level and wave conditions at two point locations in the surf zone was used to analyze the relationship between wave conditions and ripples on the bed. Values for significant wave height, peak period, skewness, ripple height and ripple period were found over bins of 15 minutes in length. It was found that there are relationships between ripple height and wave height, wave skewness and ripple height. These correlations are strongest for a zero shift in the signals, meaning the ripple height can adjust to the wave height and/or skewness within 15 minutes. These results can be used with further research, which includes local current measurements, to make more accurate estimates of the ripple height.

Contents

1. Introduction

The ocean floor is not flat; there are many different scales of topography, from mountains to formations comparable to dunes and from sand bars to ripples. This paper will focus on the smaller formations, which have heights around several centimeters and wavelength around decimeters, called ripples. Ripples occur in the nearshore under shoaling and breaking waves and are important for modeling the nearshore and surf zone because they impact the roughness of the bed (Lacy et al 2007, Grant and Madsen 1982). Aside from roughness impacts, ripples and other bedforms can be important in the transport of sediment in the nearshore (Wengrove 2018, Wengrove et al 2018, Grant and Madsen 1982). Ripples are formed by the oscillating water motions caused by waves and by currents. Many lab and field studies have focused on observing these ripples, characterizing them and relating them to the surrounding hydrodynamic conditions.

The purpose of this project was to use field data from the Sandmotor, located on the coast of the Netherlands near The Hague (Figure 1), to determine sand ripple characteristics and relate them to wave parameters such as height, period, skewness and asymmetry. Data of the bed and water levels were gathered during a field campaign in Fall 2019 for the TU Delft course *Fieldwork in Hydraulic Engineering*. Four poles were installed in a line perpendicular to the coast, at four different locations in the surf zone (Figure 2). The two poles located farthest offshore are the ones used in this study (Figure 3). The farthest offshore location, S2, was located a half-meter below the low tide on the day of installation. The second, S1, was located 5 meters inward of that pole and just below the low water line. The sediment at this location is predominantly sand with a diameter of 300 microns. Water level was measured with pressure sensors and bed level with echo sounders. Both types of sensors were mounted to the two poles located in the surf zone.

The sensors used to measure the bed level were EA400 Echologgers (generically referred to as echo sounders). In other field experiments, sonar equipment has been set up to take whole field measurements (e.g. Wengrove 2018, Dingler 1977, Traykovski 2007). However, the measurements of those field experiments were taken at larger time intervals (30 minutes to hours) than this experiment, which measured at 1Hz.

Figure 1: Location of the Sand motor on the Dutch coast, and location of the cross section. Note the orientation, the cross section faces the North-west.

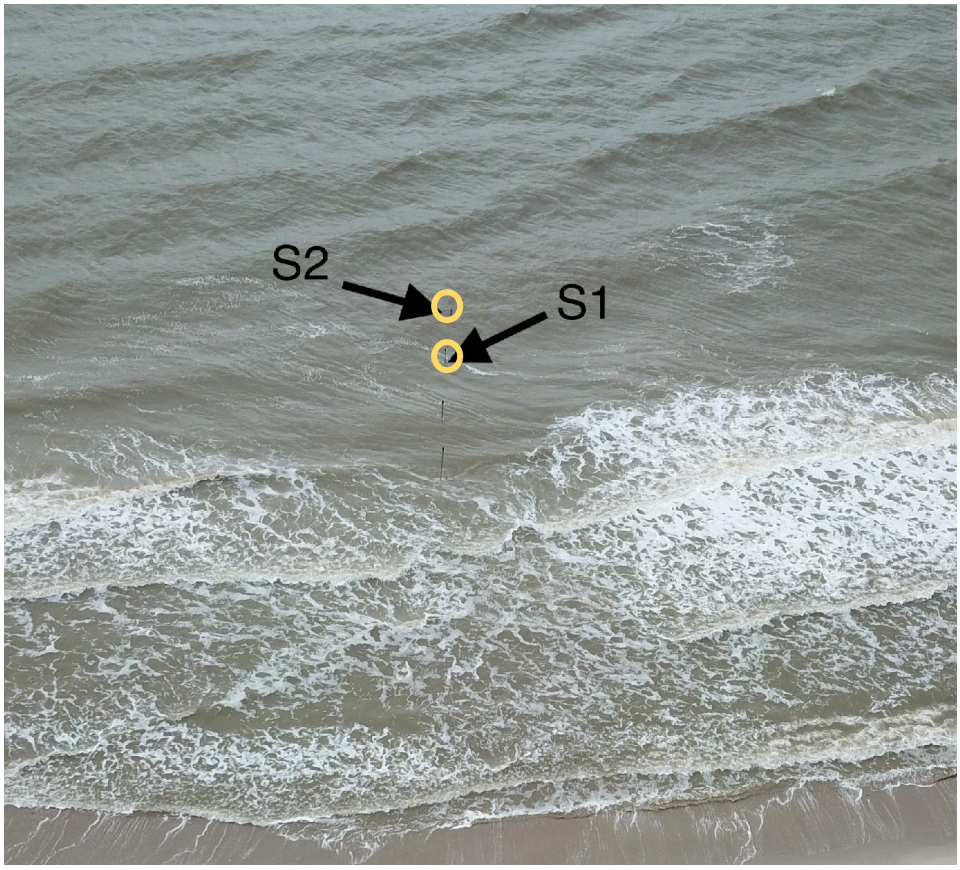

Figure 2: Locations of the echo sounders and pressure sensors, photographed from a drone during high tide. Four poles were installed during this field campaign, the data from the echo sounders and pressure sensors installed in the two offshore poles was used for this study. With the array facing approximately Northwest, this means the incoming wave direction is Southwest-west.

Figure 3: Set up on each pole used during this study. The yellow device is the pressure sensor, indicated with the blue arrow, the black the echo logger indicated with the black arrow. The farthest two offshore poles are used. The sensor pictured here was above water for too much of the time, and had a slightly different echo sounder. However, the general set up was the same at each of the poles

The echo sounders and pressure sensors were attached to a rig that was placed onto a pole (Figure 3). This was located at an initial height of 0.3m above the bed for all poles. The echo sounders were placed facing downward and recorded a 3cm diameter directly below the face. The pressure sensors were placed with the sensor on the bottom, almost level with the face of the echo sounder. Because the points from which both sensors were taking measurements were close but not exactly in line, the differences between the faces of the two sensors were taken into account. From this set up, a picture of the entire water column with the free surface and bottom as boundary can be made.

Wave data was gathered continuously at 8Hz over five tidal cycles between the afternoon of the 24th of September, and the morning of the 27th. This was gathered in the form of pressure above the RTK pressure sensors. Bed data was gathered at 1Hz for four tidal cycles, two from the 24th until the 25th of September, and another two from the 26th until the 27th. This results in two sets of data, each of two tidal cycles, for two locations. These will be referred to as S1a, S1b, S2a, S2b, with ’a’ indicating the first two tidal cycles and ’b’ the last two.

The questions to be answered in this report are as follows:

- What are the amplitudes and time scales of sand ripples?
- Do these change in response to changes in wave parameters?
- What are the general patterns in ripple and wave characteristic? Are there similarities between the two? If so, are there time lags?
- Can wave data be used to predict ripple parameters, height, or time?

2. Theory

This paper deals with two data sets, one hydrodynamic and one sediment. The hydrodynamic data consists of the pressure recorded by the pressure sensor, which was converted into a time series of the water height above the face of the echo sounder. The sediment data consists of back scatter collected by the echo sounder, which was converted into a time series of the distance to the bed from the face of the echo sounder.

As waves propagate from offshore into the surf zone, the depth changes and the shape of the wave changes until the wave breaks. Deeper water allows for bigger waves, while shallower water means smaller waves, as the larger ones break sooner. The change in depth also changes the interaction of the waves, with the bottom through friction and in turn how the bottom responds.

2.1. Waves and sediment transport

In deep water (more than one half the wave length of the wave considered), wind waves do not feel the bottom. This means there is no direct interaction between the two. As these waves propagate into shallower water, the orbital motions of the water start reaching the bottom. Bottom friction now effects the behavior of the waves. Waves in shallow water will refract, shoal, and subsequently break. (Bosboom and Stive 2015).

Refraction is the process by which waves coming into the shore at an angle rotate to become parallel to the shore. The first point along the wave crest to reach shallow water slows down because of bottom friction, the next point catches up and then slows down, and so on. Most of the time waves will begin breaking before they rotate all the way, and this leads to differences in pressure and shear stress which drive currents. Shoaling of waves is also driven by friction. When a wave enters shallower water, the front of the wave interacts first with the bottom and slows down and the rest of the wave catches up with it. This leads to a steeper wave face (vertical asymmetry), and also a horizontal asymmetry or skewness where the crest of the waves become shorter and the troughs longer (Figure 5). The speed of the wave in shallow water reaches the shallow water limit, $\sqrt{gh}$. Where g is gravity (9.81 m/s2), and h is the water level or depth which varies over the phase of the wave as h=MSL+-eta, where eta has a maximum/minimum value at +-a, and a is the wave amplitude (Figure 4). This means that the water at the crest of the wave moves quicker than the water at the trough. This asymmetry in the velocity leads to an important mechanism for sediment transport called Stokes' drift. This is the transport caused by the difference in onshore and offshore velocities (Bosboom and Stive 2015).

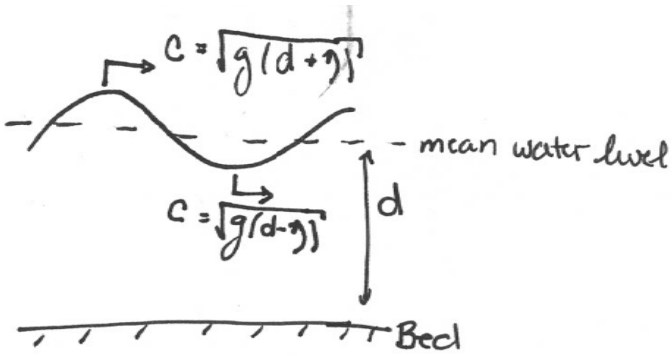

Figure 4: Illustration of the different wave speeds at crest and trough. D is the distance between the bed and mean water level, c is the wave speed, g is gravity, \eta the surface level.

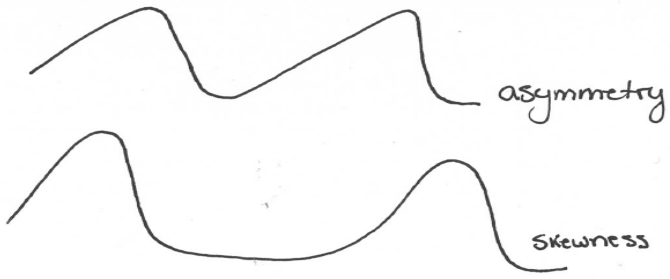

Figure 5: Wave shapes corresponding the asymmetry and skewness. Asymmetrical waves have a steeper face. Skew waves have longer troughs and shorter crests

2.2. Ripples

There are two types of sediment transport, suspended load and bedload. Suspended load denotes transport in the water column, and bedload indicates sediment moving along the bed. Ripples are a form of transport that can move a lot of sediment along the bed (Wengrove 2018, Wiberg 1994, Grant and Madsen 1982), as much as 450 wheel barrows of sand as estimated by Wengrove (2018).

Ripples are formed by the oscillating flow under waves. The regime in which ripples form starts when flow conditions are strong enough to cause initiation of motion of sediment at the bed. The upper limit is determined by the conditions which cause sheet flow. Sheet flow is when multiple layers of the bottom sediment are in motion which damps ripple formation and can wipe out existing ripples. The threshold for this is defined by a shields stress of 240 (Dingler 1977). The Shields stress (θ) is a stress normalized by sediment parameters, ρs is the density of the sediment, ρ the density of water, g gravity, D a sediment diameter, and τ the shear stress. Aside from ripples caused by the existing flow conditions, there are also those which were formed under previous conditions which could be present if the new conditions could not reform them. These are called relic ripples (Traykovski 2006, Dingler 1977, Wiberg 1994). This means that the bed at any given moment in space is a function of the present and the past conditions.

$$\theta = \frac{\tau}{(\rho_s - \rho)gD'}$$

For the basic ripple behavior, consider only one wave condition with no other currents. The shear stress caused by the change in direction of the flow stirs up sediment, which is then transported forward under the crest, or backward under the trough (Figure 6). In shallow water, the velocities under crest and trough are not equal leading to more transport under the crest than the trough (Bosboom and Stive 2015).

The instability mechanism by which ripples form is poorly understood. Once formed, they can reach an equilibrium, which is when the ripple steepness (height over wavelength) is at a maximum. Under waves alone this is the maximum steepness which can be achieved by the

material, the angle of repose (Nielsen 1981). When the bottom friction increases and conditions go beyond the equilibrium state, the steepness decreases by a decrease in height. If conditions further increase beyond the threshold for sheet flow, the ripples are wiped out and the sediment which they were comprised of transported elsewhere (Grant and Madsen 1982).

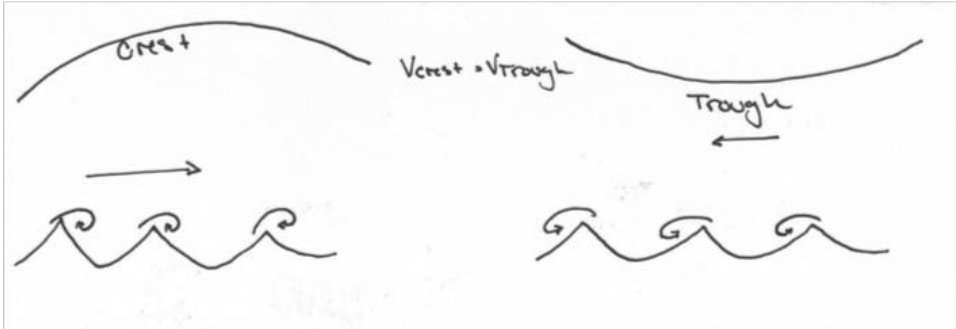

Figure 6: Theoretical flow under waves and the resulting motion of sediment at the bed, assuming the velocity under the crest is equal to that under the trough. During the crest of a wave the water moves onshore. At the bed this causes sediment to be stirred up and moved forward. During the trough the opposite happens, the water moves offshore so sediment is stirred and moved backward. When these are equal nothing changes and sediment is just moved back and forth.

2.3 Past research

Many experiments with sand ripples have gathered data in laboratory settings, some have looked at only oscillating flow (Ribberink 1994, Carstens 1969) and others at both a steady and an oscillating flow component (Lacy et al 2007). These papers define the geometry of the ripples based on their wavelength and amplitude. The general process in these experiments is to simulate waves and currents over a sand bed for a certain amount of time, then measure the ripple height, wavelength, and 3D aspects. These 3D aspects describe how long a ripple crest is as well as if the crests are parallel or branching. Due to the nature of the data gathered in this experiment (point, not whole field), neither wave length nor 3D aspects can be determined. Field experiments have mainly focused on looking at the evolution of the bed under constantly changing conditions.

Lab experiments have looked at how ripples are formed under certain wave conditions and look at a sort of equilibrium state (e.g. Lacy et al, Donoghue and Clubb 2001, Mogridge 1993, Davis et al 2004, Faraci and Foti 2002). Experiments by Lacy et al (2007) generated ripples using currents and waves. The results show that in mild currents, ripples develop in time until they reach an equilibrium of around 50-100 wave periods, which with 12 second periods is approximately 15 minutes. The ripple amplitude and wavelength grow from the flat bed and then decrease in time or stay constant depending on the magnitude of the bottom velocity. For larger bottom velocities, the wavelength increases in time while the amplitude decreases. Results also show that 3D aspects are related to the angle between the wave direction and the current direction. The smaller the angle (the smallest tested was 45 degrees) between waves and currents, the shorter crested and more 3D the ripples become (Lacy et al 2007). Looking at ripple formation and measuring at the end misses the fact that in nature the hydrodynamics are constantly changing,

and ripples may not reach the same shape found in a lab. Davis et al (2004) summarizes the time to reach equilibrium from two other studies; one that looks at whole field conditions and the other at individual ripples. For the whole field (Marsh et al 1999), the time to reach equilibrium is 30-40 minutes. While for the individual ripple (Faraci and Foti 2002), this is closer to 15 minutes. Davis et al (2004), find the time for the full bed to reach equilibrium is around 60 minutes. Though from the plots presented in the Davis et al (2004) paper, it can be seen that the initial adjustment period takes around 15-20 minutes and after that very little actually changes.

Field experiments have used sonar to look at the bed (e.g. Wengrove 2018, Gallagher 1998, Dingler 1977). Two of these studies used scans of the entire surrounding seafloor (Wengrove 2018, Dingler 1977) with sideways-mounted or rotating sonar devices, while Gallagher (1998) used a set-up of several downward facing sonar devices placed closely together (60cm) to follow migration of large scale features. This study found larger ripples (mega ripples) on the order of .1 to .5m, and observed the bed over a period of 6 weeks. The close spacing of the sensors allowed for the ripples to be tracked as they moved from under one sensor to another, and from this migration rates could be calculated. For these large ripples, the migration rate is around .1 to 1.7 meters per hour, as well as a reaction time of the ripples to changes in the flow field of about 3 hours (Gallagher 1998).

3. Processing

Something that distinguishes the data set presented here from the papers mentioned above is that only one point in space is measured. This makes it difficult to compare this data to other data sets which measure ripples. However, this data set also has a much higher frequency allowing for detailed comparisons between the bed and waves in time. The time scale of the evolution of individual ripples can also be followed using this high frequency sampling approach.

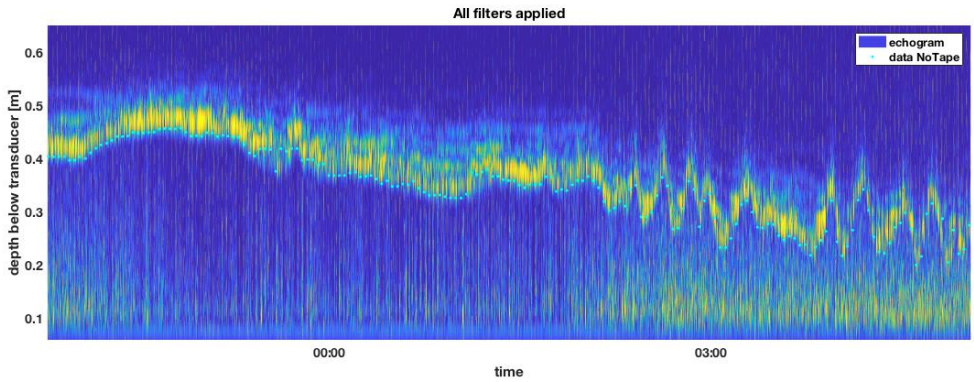

Figure 7: Segment from sensor S1 showing the backscatter from the echo sounder with the bed level points selected after filtering. The y axis shows the distance to the bottom from the sensor. The color in the backscatter plot shows the return intensity of the signal. Yellow is most intense, and blue least intense. The bottom of this band of intense return is chosen to be defined as the bed because it is the first surface that the signal bounces back from, and the method of defining the bed consistently returns points which correspond to the bottom of this band.

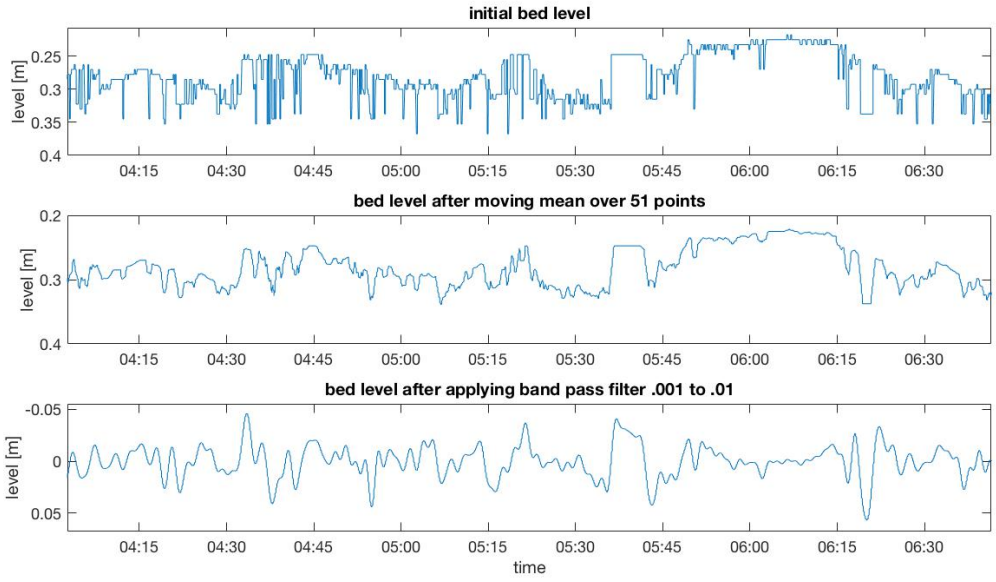

Figure 8 Stacked examples of different filters used to filter the bed level. Note that the y axis of the third subplot is not the same as the others since it is not the absolute bed height but the oscillation around a mean. For both filters, the quick and big oscillations, which look like lines in the top plot are filtered out. The moving mean slightly damps the height of the ripples, and returns a blocky signal. The band pass filter returns a smoother curve, and ripples of a longer time scale, such as the one between 5:45 and 6:15 are filtered out.

3.1 Echo sounders

The backscatter returned from the echo sounder gave the bottom depth as distance to bottom from sensor. To choose a single value, 10 backscatter arrays were averaged, and the depth with the sharpest gradient in number of returned pings per distance was taken as the bottom. All of these bottom points represent the time series of the bed (Figure 7).

Ripples were defined by finding the local minima and maxima in the bed signal; these are the troughs and peaks (figure 9,10). The ripple amplitude is then the difference between a crest and its preceding trough. This is similar to the zero-crossing method used to define waves, except that instead of using the zero crossing as the start/end of each wave (ripple, in this case) the troughs are used. This eliminated the need to define a zero line. The ripple period is then taken as the time between two troughs, by multiplying the indices between troughs with the sampling frequency (56/60 Hz). This method will hereafter be referred to as the peak-trough method.

Several methods for filtering the data for ripples were tested. The first was using only the moving mean (Figure 8). The number of points over which to take the mean was determined by trial and error, and a value of 51 was settled on. This value removed what was thought to be wave noise at low tide, while maintaining the smaller ripples and not damping the amplitudes too much. The second method attempted was a combination of moving mean and low pass filter. This was not successful, as it was not able to filter both the higher and lower unwanted frequencies. The third was a combination of moving mean as before, and a bandpass filter as used by Davis et al (2004). This allowed for a certain range of frequencies to be focused on. The other benefit of the bandpass filter is that the resulting bed level fluctuated around a mean, meaning only the ripples were retained and none of the longer scale oscillations (Figure 11). This also makes the peak-trough method of defining ripples more

accurate (Figure 10) than previous application to the signal filtered by solely the moving mean (Figure 9). The limits for the band pass filter were chosen based on a combination of wave frequency and trial and error. The upper limit should be around the wave frequency, since these two spectrum are being compared. The long wave frequency for this dataset was around .02 and through trial and error it was found that an upper limit of .01 resulted in a good signal. The lower limit was determined with trial and error, the aim was to remove the larger trends in the bed data (Figure 8, Figure 13). These were not of interest, since their scale is much longer than that of the waves, and the filter to look at only these long oscillating, a band pass looking at lower frequencies, did not create a very reliable match (figure 11). A lower limit of .001 was ultimately chosen, so all ripple periods analyzed lie between 100 s and 1000 s.

3.2. Pressure sensors

The pressure sensors return a time series of pressure data. Scripts provided with the sensors converted the raw data to pressure in time. Other scripts which were provided were used to calculate the wave spectrum and parameters such as height and period from the pressure signal (see appendix for list of scripts and their functions). The "depth to bed" for the wave calculations was defined as the mean of the bed level plus the difference between the faces of pressure sensor and echo sounder, as opposed to using the value measured during installation of the devices.

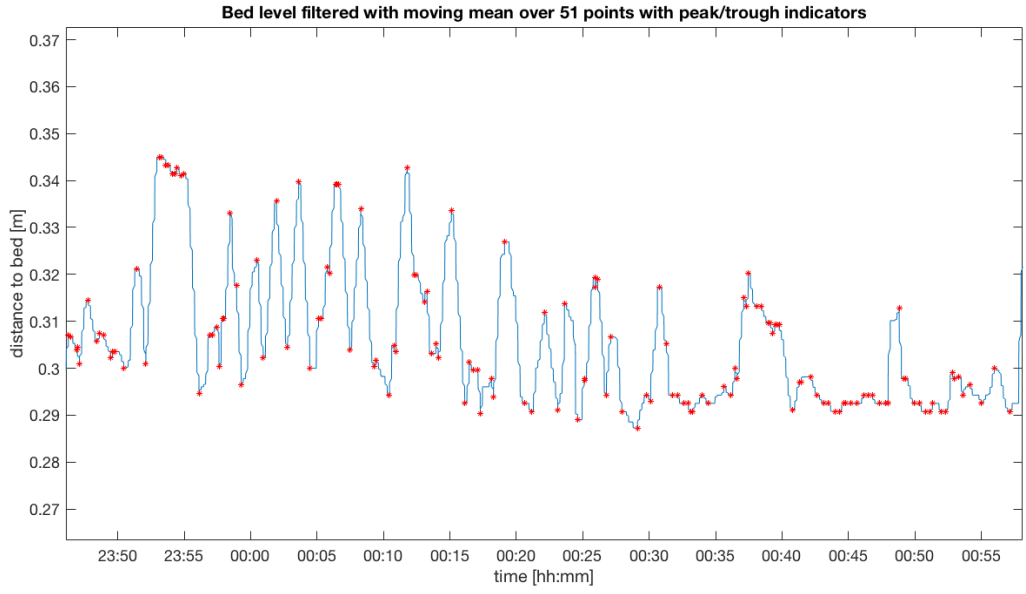

Figure 9 Example of how peaks and troughs of ripples are defined on a portion of the signal filtered with a moving mean. The red stars represent the points which are defined as the peak or trough. Note that the blockiness of the signal leads to several peaks and troughs defined at the same level, for example the crest just before 23:55 and the segment just after 00:45 have many peaks and troughs indicated where there do not appear to be significant ripples.

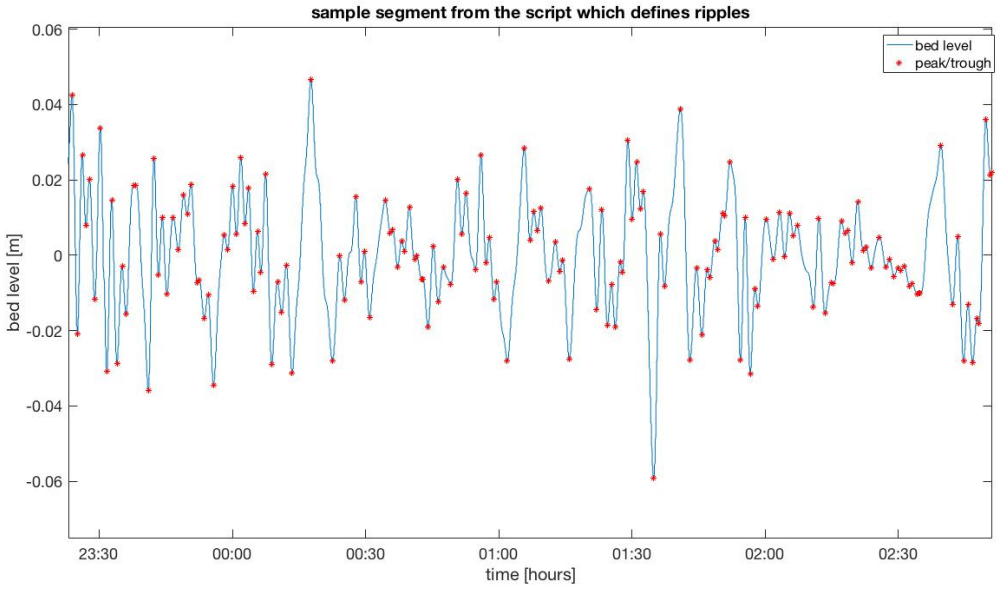

Figure 10 Shows how peaks and troughs are defined on a portion of the signal filtered using the bandpass filter with limits .01 and .001. Note this is not the same section as used in figure 9. Each peak and each trough are defined with one point each, unlike for the segment filtered with the moving mean. Note that the peaks and troughs defined by the script now match visually to what would be expected to be a ripple. There are no double defined peaks as there were for the moving mean filtered signal.

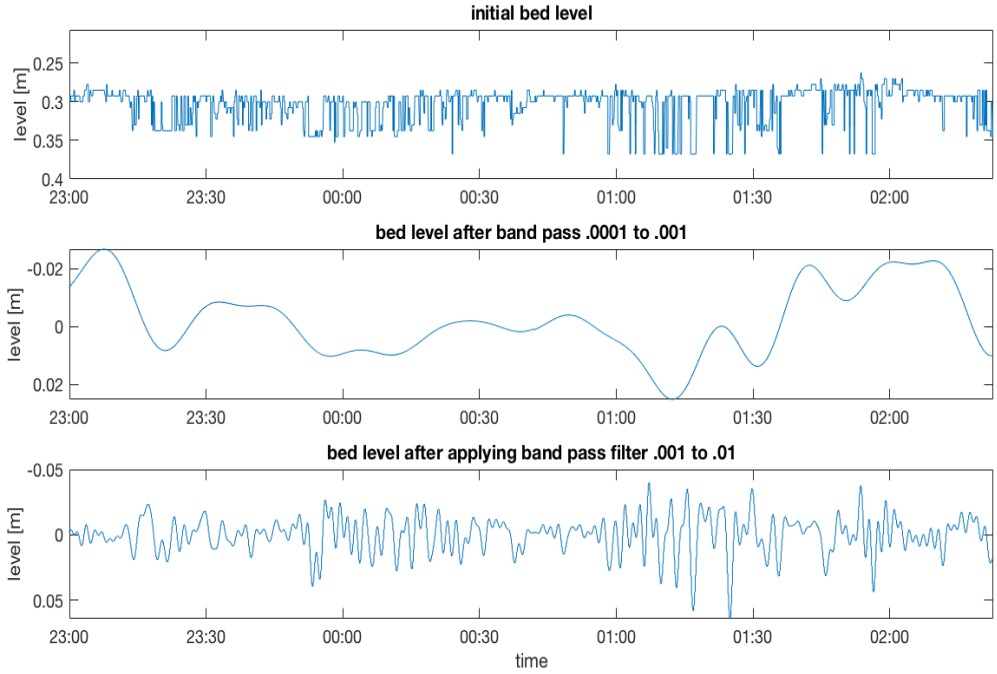

Figure 11 To test whether the limits on the bandpass filter showed the ripples that were wanted some frequencies were compared. The top plot is the unfiltered bed level. The second plot is filtered to show the longer period ripples, these are much smaller than the higher frequency ripples, and also do not really resemble what is seen in the signal. The third plot shows the bed filtered to the higher frequency ripples The section chosen to demonstrate this is a tricky one as there are a lot of high frequency motions, but for both this section as the entire dataset it does appear that the .001 to .01 frequency band is the appropriate one to look at.

These two data sets were gathered at a different frequency, the wave data at 8Hz and the bed data at 1Hz. This 1Hz was actually 59/60Hz, which will be rounded when mentioned in this report but all calculations were done using the real value of 59/60. Several options were available to match the data. One was to sub-sample the wave data, which at 1Hz would have led to problems with aliasing and misrepresentation of the wave conditions. Another was to interpolate the bed data to 8Hz, which due to the bed data being sampled at an odd integer led to issues with extrapolation. The last was to calculate and compare parameters in blocks of a certain time, and not extrapolate or sub-sample either set. The first method was not used at all, and the second method was attempted with mixed success. The interpretation is possible, and works for small blocks of time. For longer series of data the time becomes increasingly shifted. The last method was the one finally chosen for the data represented in this study. The second method of interpolation would be appropriate for looking at instantaneous behavior, this was not our goal for this report, therefor the last method was chosen. The bed data was broken into blocks of 15 minutes, and those start and end times used to calculate the wave parameters from the appropriate sensor for that segment of time.

3.2 Parameters of ripples and waves

Much of the initial processing involved solving for a variety of parameters and visually comparing plots. The parameters calculated were for the waves:

- Wave height

  The H_1/3 is the average of the highest one third of waves, Hrms is the root mean square and is lower than the H_1/3. All wave heights which can be defined are linearly related. The H_1/3 is used in this study.

$$H_{rms} = \sqrt{\sum {H_{individual}}^2}$$

$$H_{1/3} = \frac{1}{N/3} \sum_{j=1}^{j=N/3} H_j$$

  Where H and $H_{individual}$ are both individual wave heights, j is the index of wave heights sorted in descending order, N is the number of waves.

- Peak period

  Inverse of the peak frequency, which is the frequency at which the most wave energy is found

- Asymmetry

  A measure of the difference in the steepness of the front and back face of a wave, calculated with a Hilbert transform:

$$As = {Hilbert(\eta)^3} \Big/ {\overline{\eta^2}^{3/2}}$$

  Beta (β) used to represent the asymmetry:

$$\beta = \arg(As)$$

- Skewness

The third statistical moment of the signal, shows relatively how much time is spend above or below the mean. Where μ is the mean and σ the standard deviation.

$$\mu_3 = \frac{\mu^3}{\sigma^3}$$

And for the sand ripples:

- mean and peak period
  Periods were defined as the time between two troughs. The peak is the maximum value and the mean is the average over a defined time scale
- mean and peak ripple height
  Ripple height was defined as the difference between a peak and the preceding trough. Same as for the period, the peak is the maximum and the mean the average

To compare these parameters, the peak and mean values were found over bins of several minutes. It was found that any bin less than 8 minutes led to errors in defining ripples since at least one ripple (trough-peak-trough) had to be present in the bin for the script to run properly. Using binned data also means that the instantaneous (within seconds) effects of the waves on the bottom cannot be seen. A bin size of 15 minutes was ultimately used, meaning there are a few ripples (2 or more) over which the average or peak parameter values are taken.

The time scale of the ripples is defined as the ripple period, the time for a ripple to pass under the sensor measured from trough to trough. Several different processes and parameters contribute to this period. When thinking of the bed as steady, only changing in space, it is a factor of wavelength and propagation speed. However, the bed forms could be developing by growing or decaying. Which means that the period includes the time scale of formation or decay of a ripple as well as its propagation. Wengrove et al (2018) determined with observations that ripples can be either moving, growing/decaying, or both.

4. Results

The results are presented in this section, they are organized by first presenting the overall wave data, then looking at the overall bed data. Then, we combine the wave and bed data and look at comparing the parameters mentioned in the previous section. Lastly, we present and analyze scatter plots of different wave and ripple parameters.

4.1. Wave data

The wave data is presented below for the full time series for each sensor, S1 and S2.

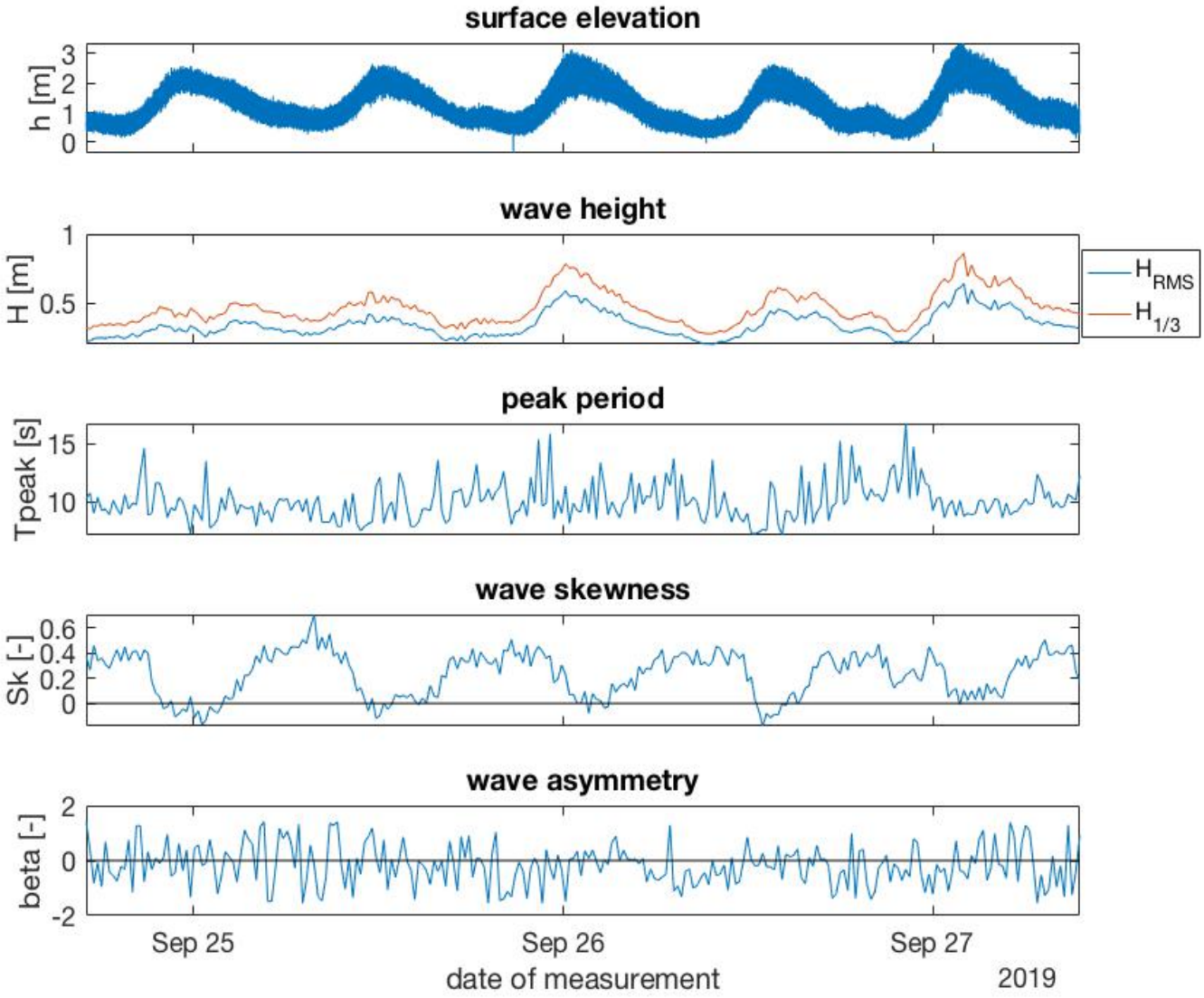

Figure 12 Wave parameters measured at S2 over five tidal cycles from the afternoon of September 24 until the morning of September 27. The first subplot is the time series of the surface elevation, including waves. The second shows two different wave heights, the root mean square (rms) wave height and the H_1/3 which is the wave height used in this report. They are linearly related. The third subplot shows the peak period, which is derives from the frequency spectrum. The fourth is the wave skewness, which is a measure of how much time the signal is above or below the mean. The fifth is wave asymmetry, a measure of the asymmetry of the steepness of the back and face of a wave. Note that both the wave height and skewness vary regularly over the tidal cycle. Also note the tidal cycle, the incoming tide occurs over a much shorter period that the outgoing. There is also an inequality, which is why at the beginning there is one peak, but the last two recorded tidal cycles have a smaller peak between the two full high tides.

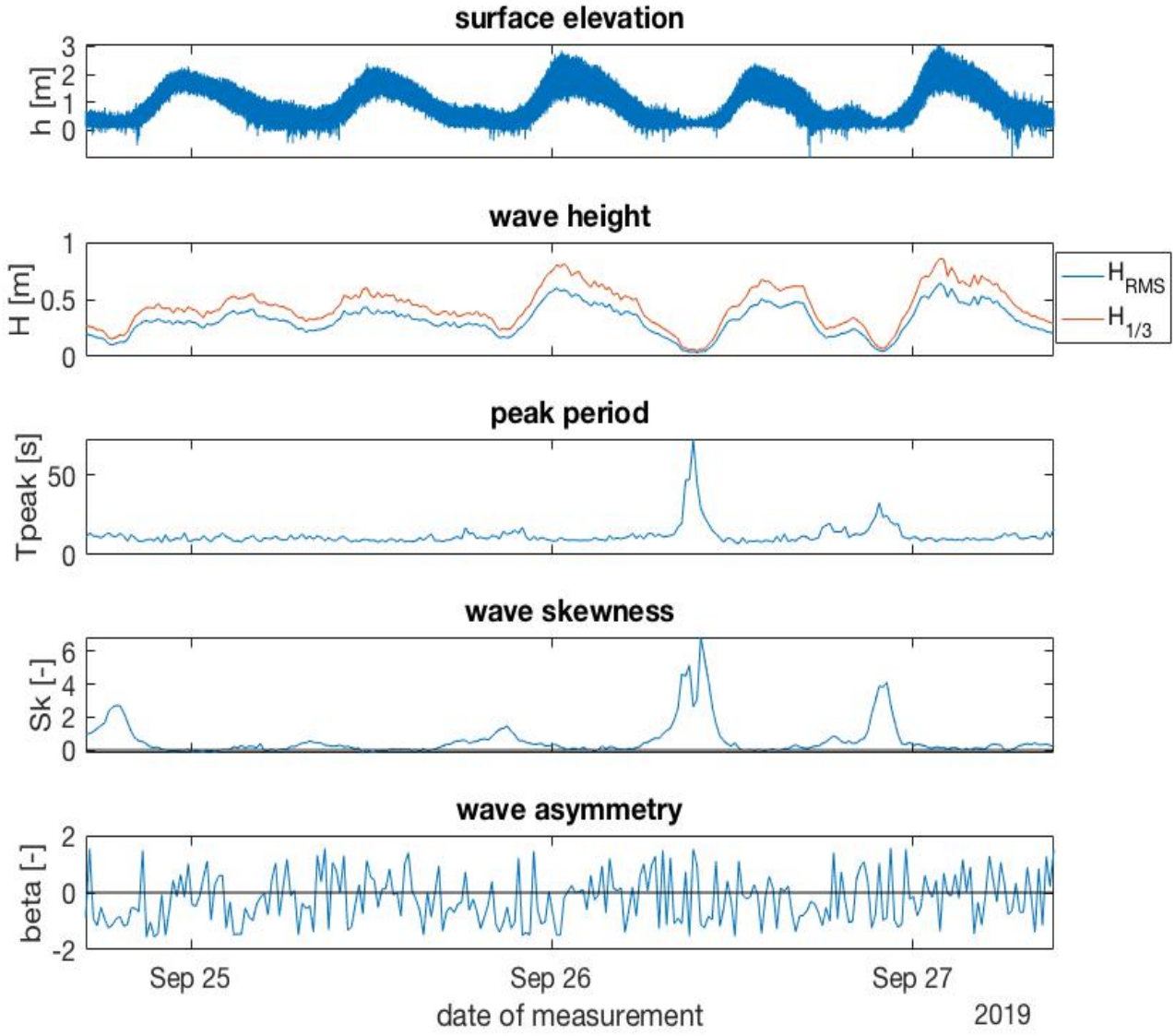

Figure 13 Wave parameters measured at S1 over five tidal cycles from the afternoon of September 24 until the morning of September 27. The first subplot is the time series of the surface elevation, including waves. The second shows two different wave heights, the root mean square (rms) wave height and the H_1/3 which is the wave height used in this report. They are linearly related. The third subplot shows the peak period, which is derives from the frequency spectrum. The fourth is the wave skewness, which is a measure of how much time the signal is above or below the mean. The fifth is wave asymmetry, a measure of the asymmetry of the steepness of the back and face of a wave. Note the peaks in the peak period and skewness plots. These coincide with very low water, meaning that the sensor was likely above water at not recording waves. The smaller peaks in the skewness are real, and as with the other sensor occur through low tide. Note in the first subplot during low tide the signal shoots below zero, this is due to breaking waves.

4.2. Ripple data

The backscatter from the echo sounders was processed as described in the previous chapter. A moving mean over 51 points was applied to clean the noise (Figures 14, 15), followed by a bandpass filter with the limits .001 and .01, removing any oscillations outside of that frequency range (Figure 16, 17). The higher frequency limit of .01 is of the same order of magnitude as the long wave frequency. The lower frequency was chosen to be just small enough to keep the signal oscillating around a mean, but large enough to include a range of frequencies. Peaks and troughs were then identified in this signal, and ripple height and period calculated for each location and time. The resulting individual heights and periods were then sorted into bins of 15 minutes and mean/peak values where the average and maximum values were takes as the mean and peak respectively (Figure 18, 19).

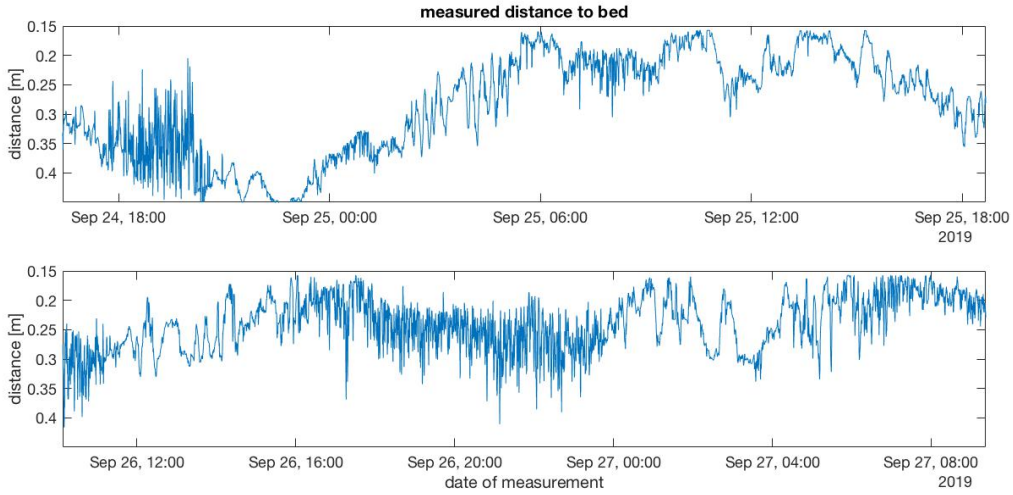

Figure 14 Full time series of bed measurements of S1, noise filtered by using a moving mean average over 51 points. The top subplot is over the first two tidal cycles, measures from the afternoon of September 24th until the afternoon of September 24th. The second subplot is the last two tidal cycles, from the morning of September 26th until the morning of September 27th. Note that there are large longer scale oscillations in the bed level, these are filtered out in the data set used for analysis in this report.

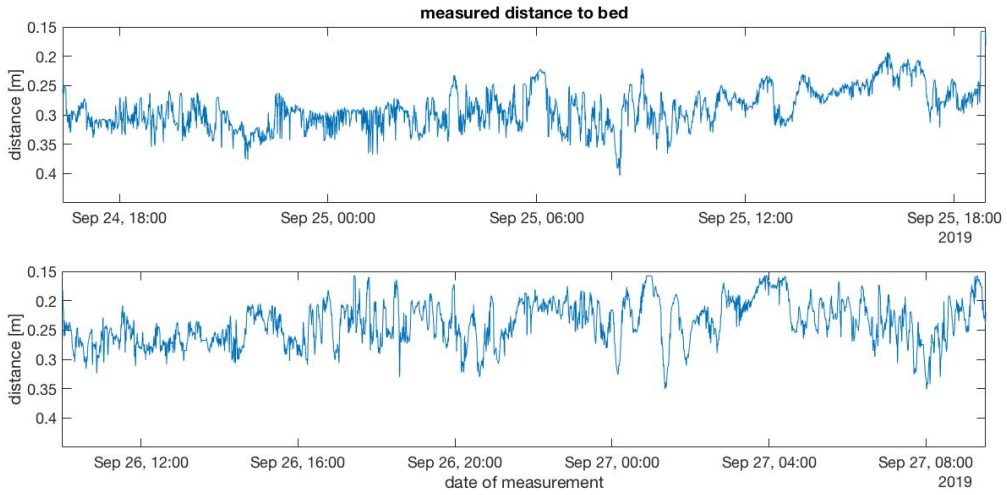

Figure 15 Full time series of bed measurements of S2, noise filtered by using a moving mean average over 51 points. The top subplot is over the first two tidal cycles, measures from the afternoon of September 24th until the afternoon of September 24th. The second subplot is the last two tidal cycles, from the morning of September 26th until the morning of September 27th.

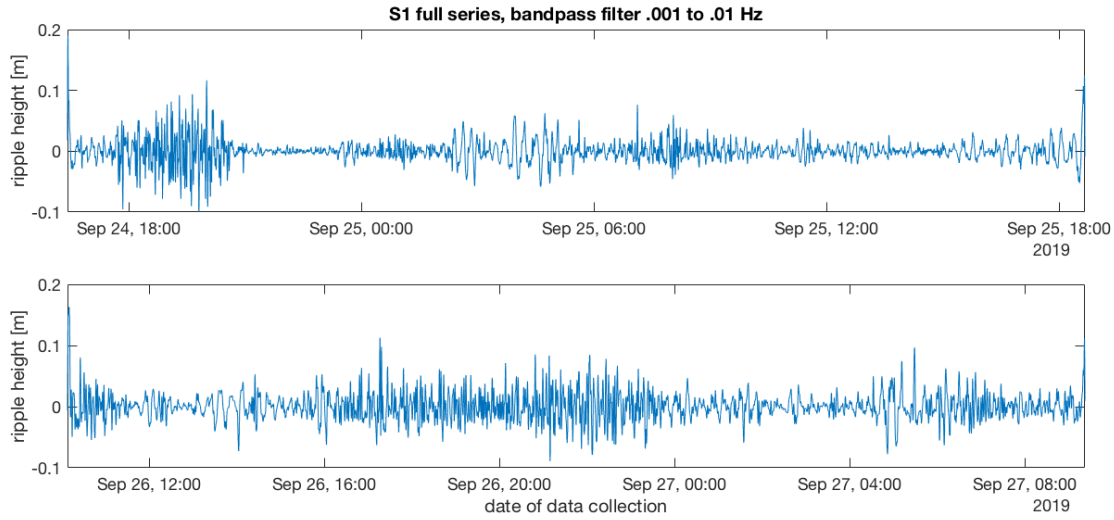

Figure 16 Full time series for S1 of the bed run through a band pass filter to select the ripple frequencies of interest, between 100s and 1000s. The bandpass filter removed the lower frequency oscillations meaning that the remaining higher frequency ripples fluctuate around a mean

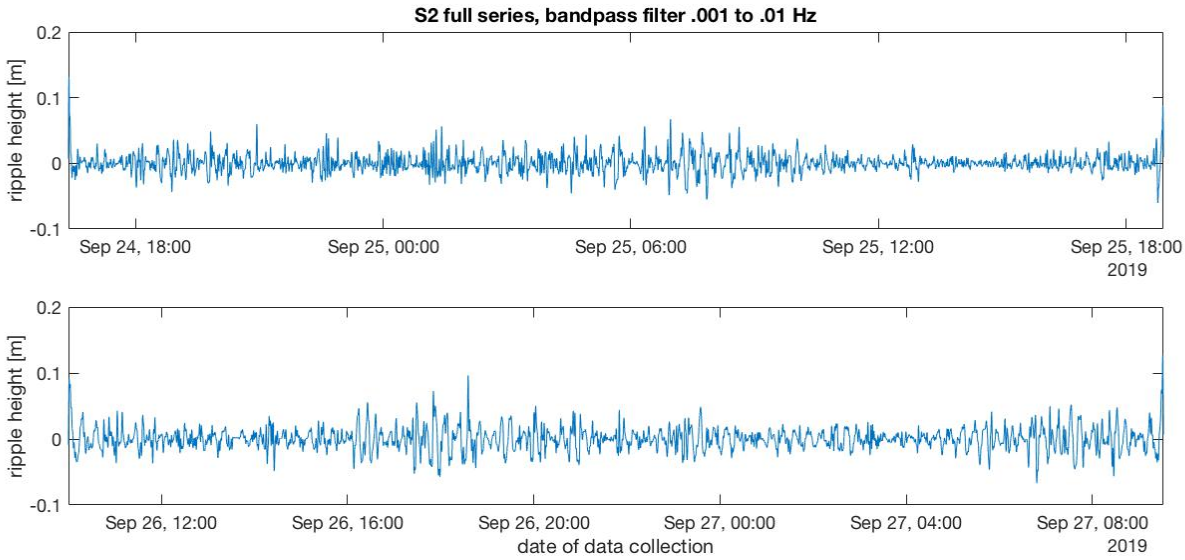

Figure 17 Full time series for S2 of the bed run through a band pass filter to select the ripple frequencies of interest which correspond to ripples with periods between 100s and 1000s.

4.3. Matching wave and ripple data

The ripple signals in figures 20 through 24 show a variation in ripple heights that appears to be on the same cycle as the tide. During higher water, the bed has a lower mean ripple height, and during lower waters a higher mean ripple height. This generally holds true. However there are times when the ripple height is not related to the water level but to the wave height (Figure

22). Since the wave height usually corresponds to the tide (Figure 12, 13), the waves being depth limited, it can appear that the ripple amplitude follow the tide when in fact it matches better with the waves.

Skewness of the waves is related to sediment transport in the general sense, Stokes drift causes transport as described in chapter 2. If ripples are a form of transport it could be that skewness also plays a role in their formation or propagation. Asymmetry is another wave parameter thought to influence the transport of ripples. At first glance, there doesn't seem to be any sort of pattern for asymmetry (Figure 24). For skewness, the strongest correlation appears with the onshore sensor S1 (Figure 25), while the offshore sensor (S1) shows a very slight positive linear trend with a low R^2 value.

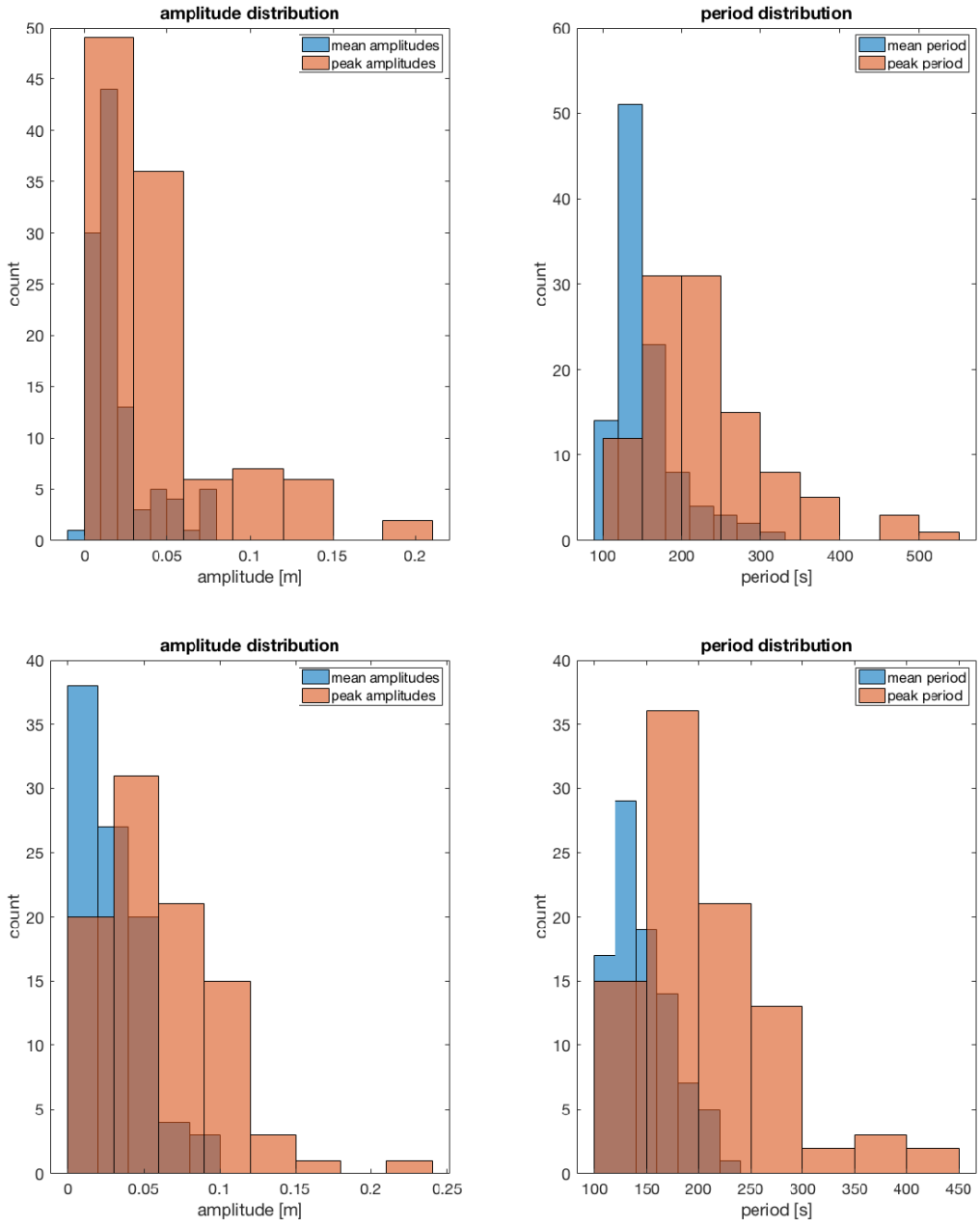

Figure 18 Histograms of amplitude and period of the bed level changes, ripples, for S1. Top row is for the first half of the dataset, bottom row for the second half. Over all the peak amplitude is around .05m, the mean around 0.1. The peak period around 200 seconds, and the mean around 150 seconds.

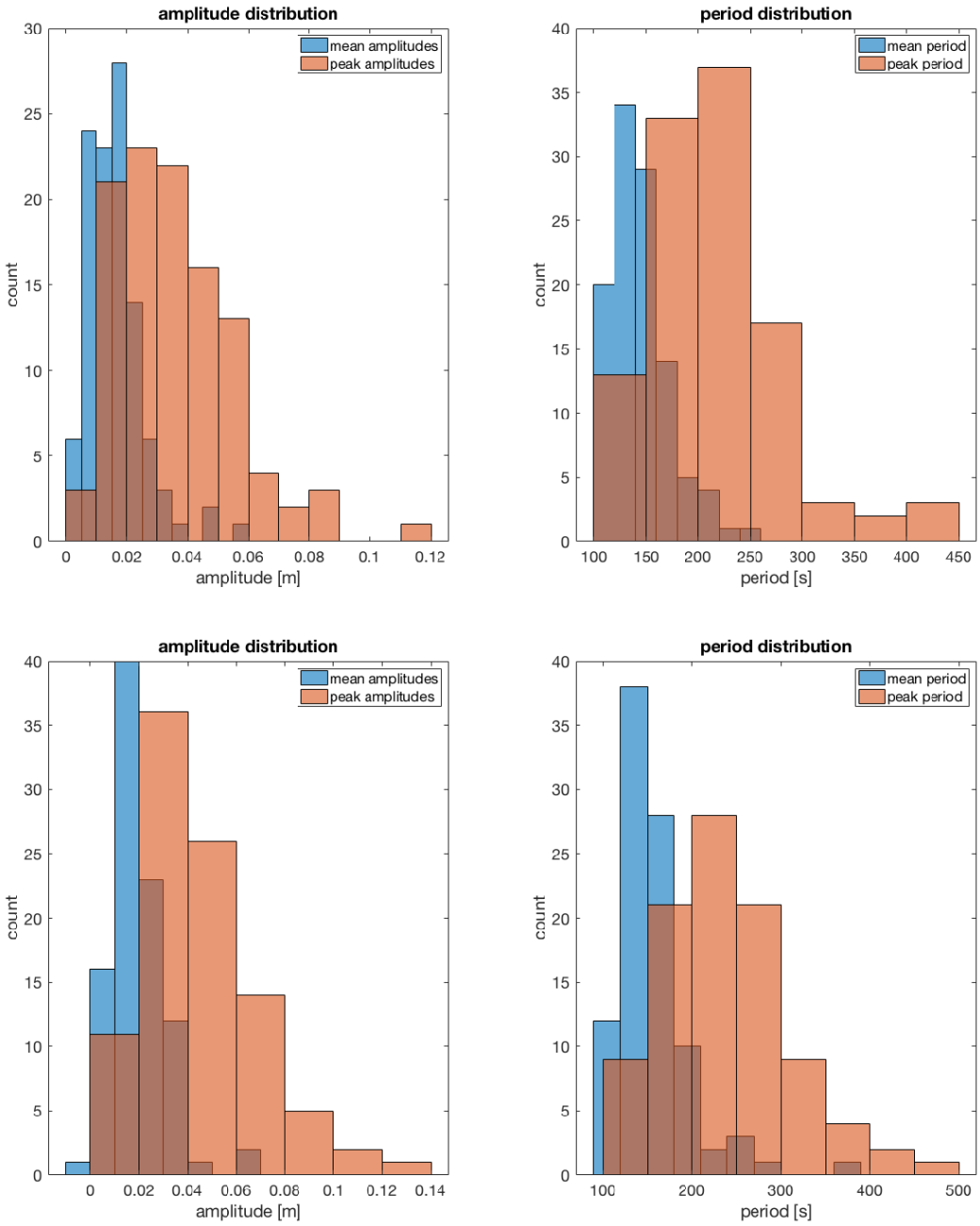

Figure 19 Histograms of amplitude and period of the bed level changes, ripples, for S2. Top row is for the first half of the dataset, bottom row for the second half. The peak amplitude is around .03m, the mean around .02m. The peak period is around 250s, and the mean around 150s.

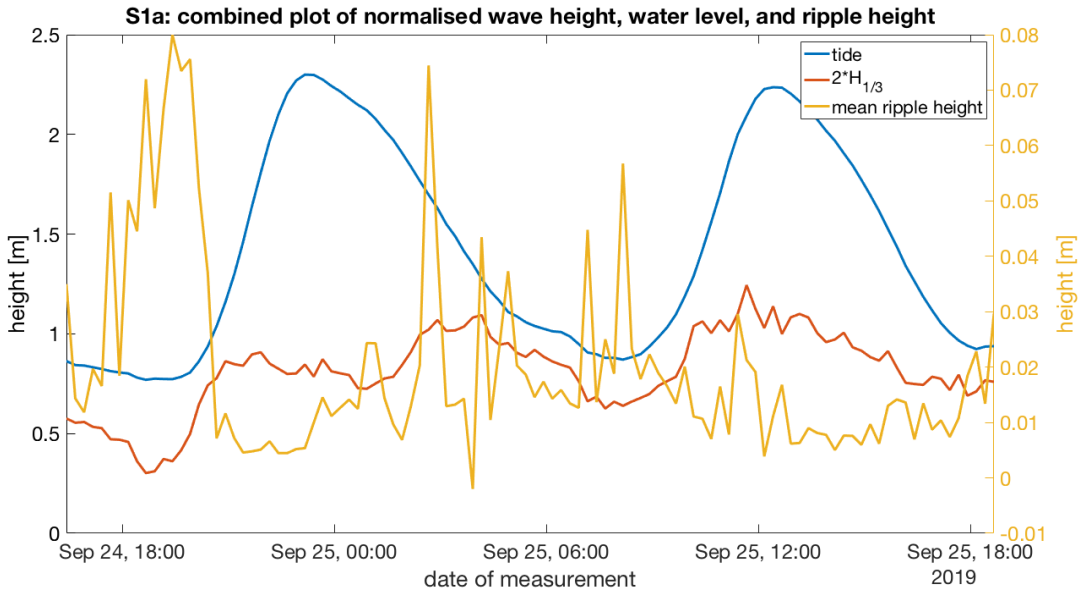

Figure 20 overlapping plot of water level (tide, blue line), wave height multiplied by a factor of 2 for visibility ($H_{1/3}$, red line), and mean ripple height (yellow line) for S1a. The lowest ripple heights occur around the highest water levels, and the highest ripple heights close to low water but there is also a peak on the first outgoing tide.

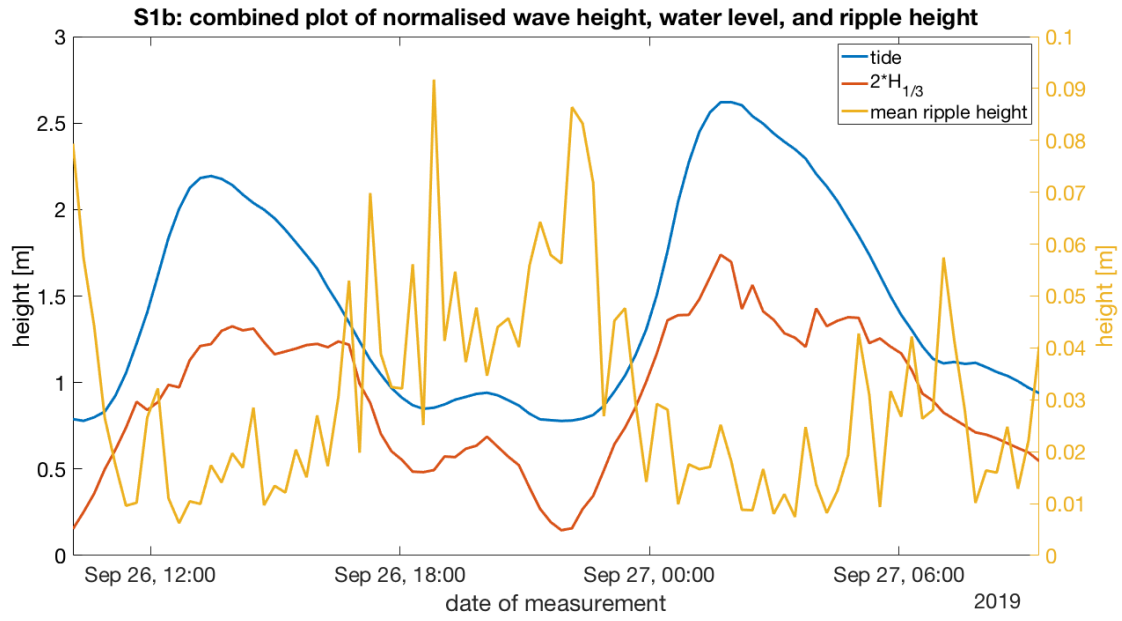

Figure 21 overlapping plot of water level (tide, blue line), wave height scaled by a factor of 2 ($H_{1/3}$, red line), and mean ripple height of the filtered bed level (yellow line) for S1b. For this plot, the peaks in ripple height do correspond with the lowest water levels and vice versa. However, there is also good agreement with the waves. There are larger waves at higher tide, and smaller at lower tide.

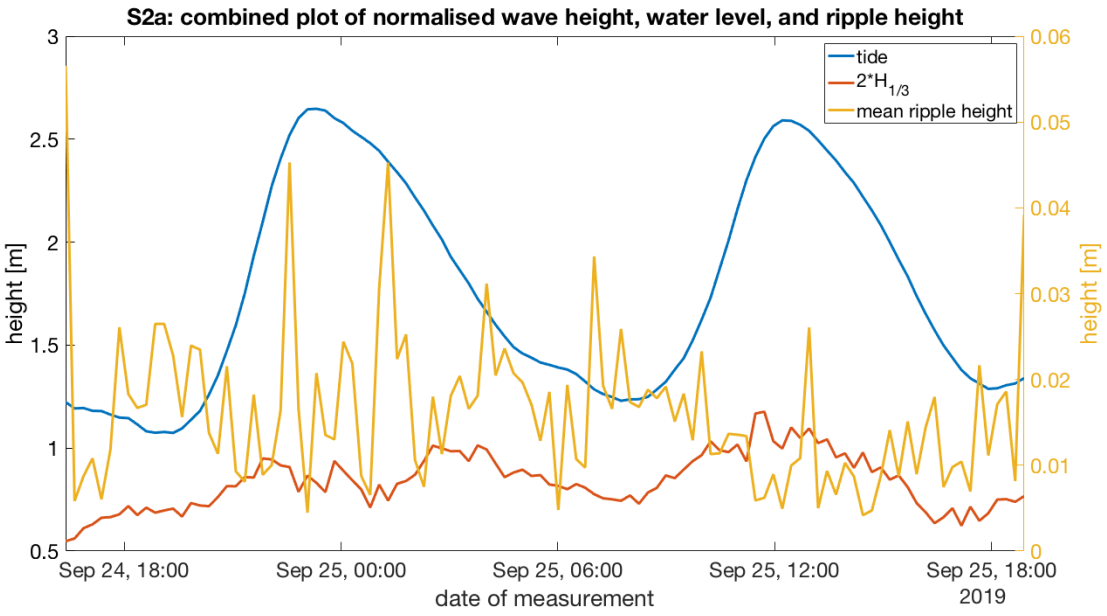

Figure 22 overlapping plot of water level (tide, blue line), wave height scaled by factor two ($H_{1/3}$, red line) and the mean ripple height (yellow line) for S2a. The wave height does not vary perfectly with the tide during this segment, neither does the ripple height. Looking at the section around 00:00 on the 25th of September the ripple height here is at its maximum for this segment. The wave heights are fairly small (20 cm) and have two points on either side of the 00:00 tick where they are smaller, with the area between them having slightly larger waves. The ripple heights have the opposite behavior, being maximum at either side of the 00:00 tick and smaller in between. This indicates that the relationship between ripple height and wave height is probably stronger than between ripple height and water depth alone.

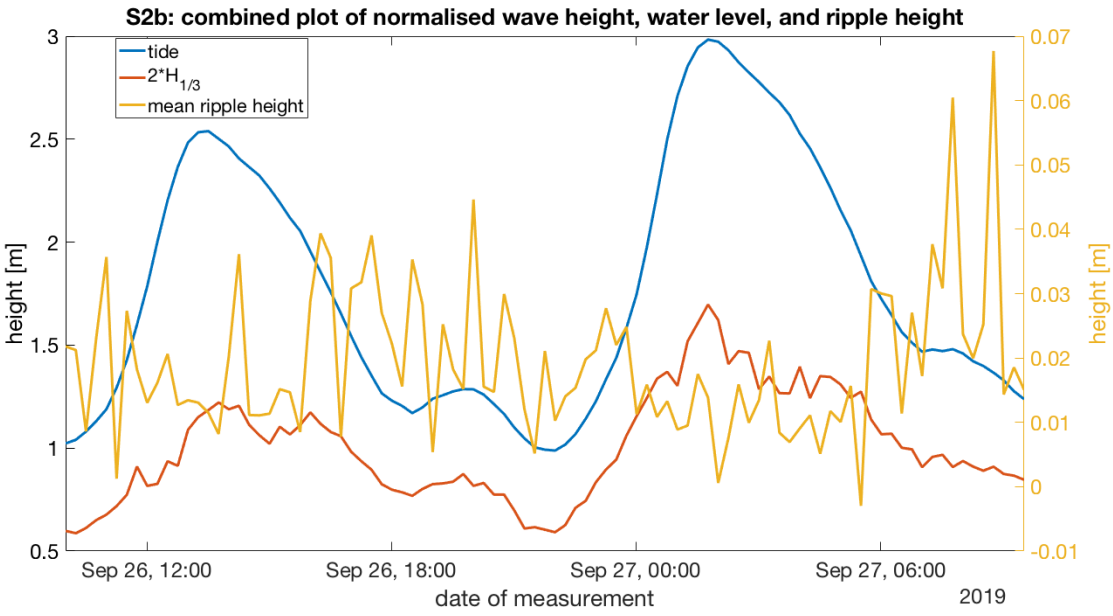

Figure 23 overlapping plot of water level (tide, blue line), wave height (H_1/3 , red line) and the mean ripple height(yellow line) for S2b. During this section the maximum mean ripple height is observed. Note that this happens around low tide with a wave height a bit below 0.5m. During the high tide prior to this maximum there are the highest waves. During this period there are also the lowest ripple amplitudes for this section.

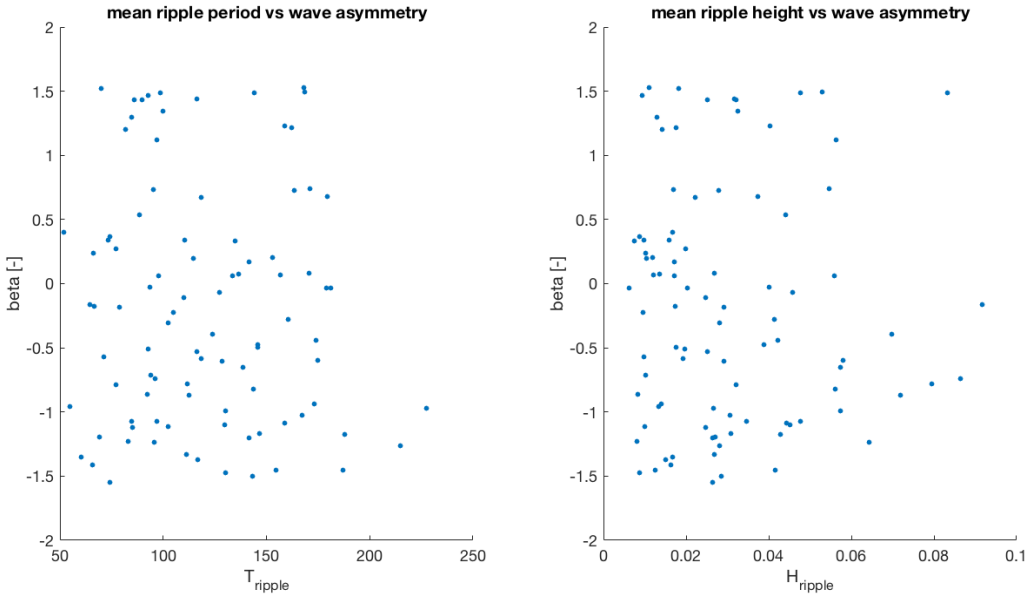

Figure 24 Wave asymmetry as represented by beta vs first ripple period and second ripple height for a sample of data. This relationship was equally scattered for all data, and there does not appear to be any sort of relationship between asymmetry and either of the ripple parameters.

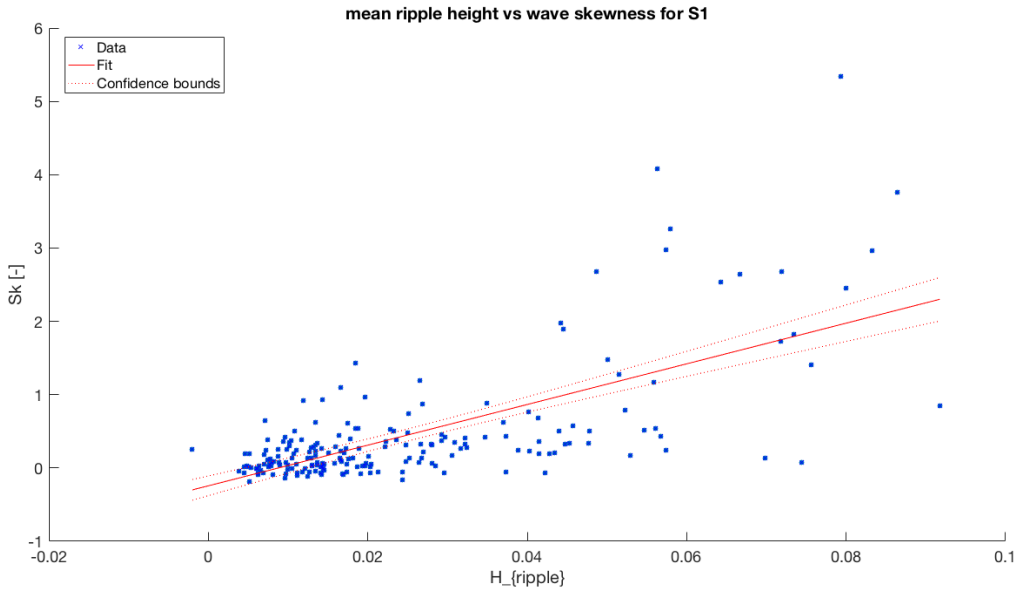

Figure 25 Mean ripple height vs wave skewness. There is a positive linear correlation present between these two parameters, with an R^2 value of .45 which is indicative of a fairly good match. This means that the more positively skewed the waves are, the larger the ripples will grow.

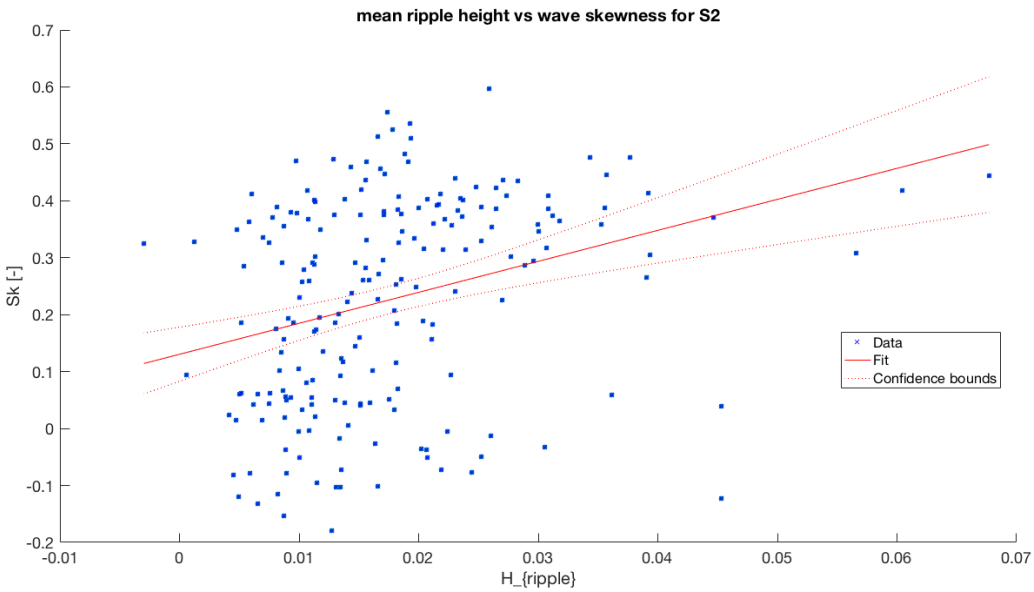

Figure 26 Mean ripple height vs wave skewness for the most offshore sensor. There is a positive linear fit but the R^2 value is quite low, .09, meaning the correlation between the two parameters is weak.

The relationship between skewness and the offshore sensor is weaker, however it is important to note the axis limits in these two figures. The onshore sensor, S1, experienced much higher values of skewness than the offshore sensor and also higher ripple amplitudes. The linear fit between the ripple amplitude and wave skewness for S1 has an R^2 of .45, which indicates there is a positive linear relationship between the values. The linear fit on the S2 values has a much lower R^2 value (.09), meaning a weaker relationship between the parameters. The strength of this correlation indicates that for the onshore sensor, the one which was located in or very close to the breaking waves the ripple amplitude grows with skewness.

In theory from the papers discussed in Chapter 2 (Dingler 1977, Traykovski 2007, Grant and Madsen 1982), the ripple heights should grow with wave height until a certain maximum where the conditions approach sheet flow and the amplitudes decrease. The idea being that it takes some energy to initiate motion and form ripples, and past a certain threshold there is enough energy to begin flattening out ripples. For the onshore sensor, S1, there is a negative linear trend, with the largest ripple heights occurring between wave heights of .1 and .3 m, and for every larger wave height the ripple height is smaller. This means that even at the smaller wave heights there is enough energy for sediment to be in motion. For S2, the trend is different (figure 27). The maximum ripple heights occur around a wave height of .4 m, with smaller ripple heights for wave height above and below that value. The linear fit is still negative but has a much lower R^2 value (.02). It takes more wave energy, larger waves, at this deeper sensor to reach the maximum ripple height. This could be due to the longshore current which is (at least in theory) stronger farther offshore by the sand bar and goes to zero at the water line (Bosboom and Stive 2015).

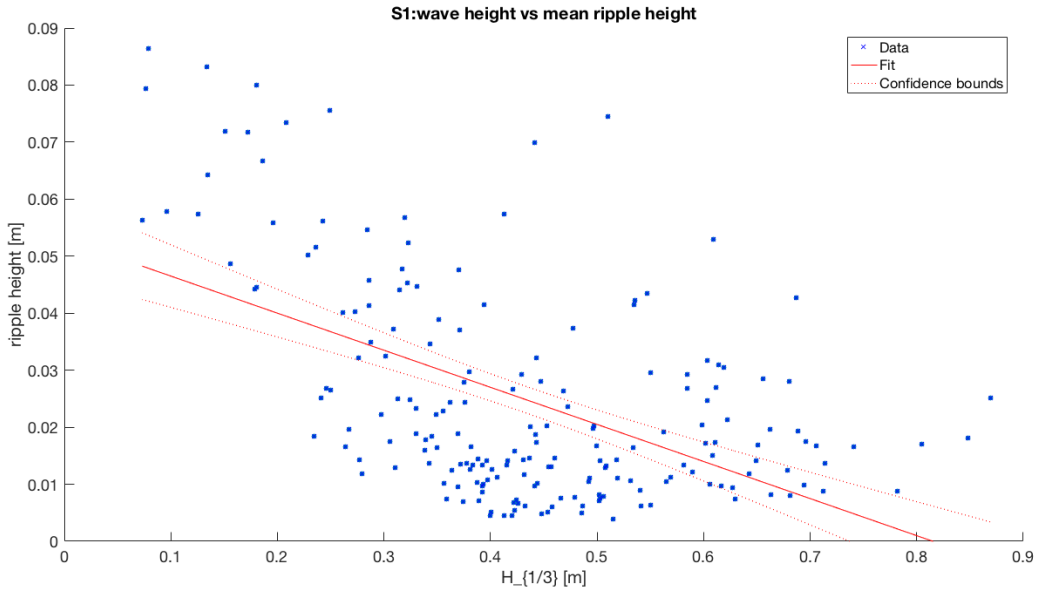

Figure 27 Scatter plot of ripple height vs significant wave height for sensor S1. The highest recorded ripple is .09m and occurs at a wave height of around .1 m. For larger waves, the maximum ripple size decreases. The negative linear fit for this set of data has an R^2 value of .27, so it is not a perfect fit but the general trend is that ripple height decreases with increasing wave height.

The ripple period is a function of propagation as well as formation. It would make sense that the formation time is related to the ripple amplitude, if larger ripples take longer to form, and these are not migrating, the trend should be positive linear (Figure 28, 29). The largest ripple heights occur at S1. These don't have the largest periods as would be expected if only formation time were being measured. There is an slight positive linear trend for both sensors, but with the confidence bounds it is nearly has a zero slope. The idea that ripples are dispersive is suggested by Jain and Kennedy (1974), and supported by Davis et al (2004). This implies that their propagation or migration speed is related to their wavelength. However, since wavelength is not available from this dataset, not much can be said in this regard and the components of the ripple period cannot be discerned. What was found however was the relationship between ripple period and long wave period, which are of the

same order of magnitude and often very similar values (Figure 31, 32). The range of ripple periods is around twice that of the range of long wave periods, though there is no strong linear relationship.

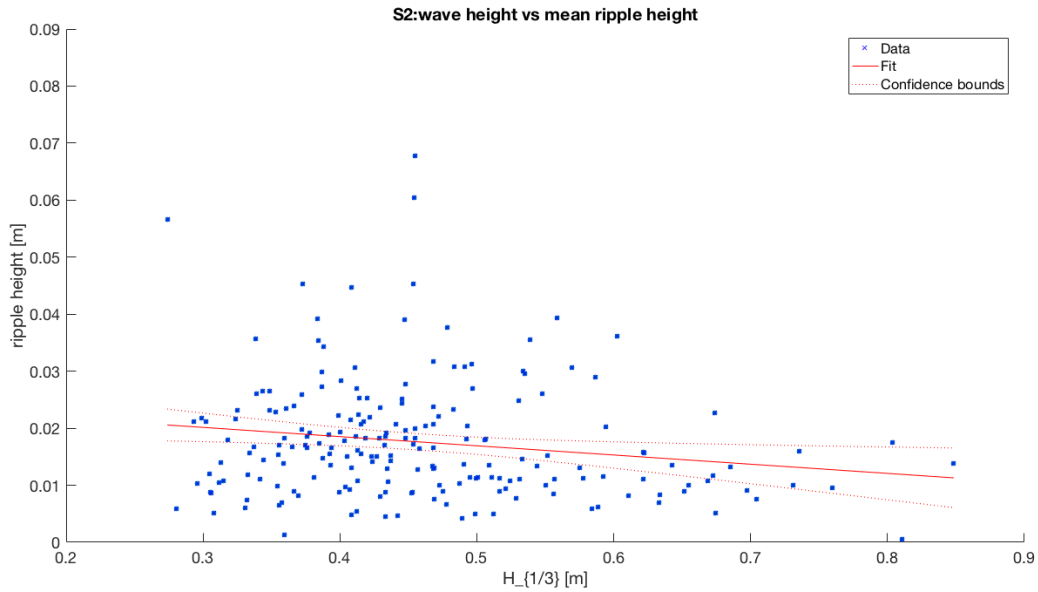

Figure 28 Scatter plot of ripple height vs significant wave height for sensor S2. The largest ripple height is .07m and occurs at a wave height around .45 m. For waves smaller and larger than this the maximum ripple size decreases. The linear fit has a negative slope, so for larger wave heights the ripples are smaller. Though small ripples are present throughout all wave heights. Another possible way to see this scatter plot is by looking at the maximum ripple height per wave length. The highest ripple heights occur between .4 and .6 m wave heights, and for wave heights smaller and larger than that the ripple heights are smaller.

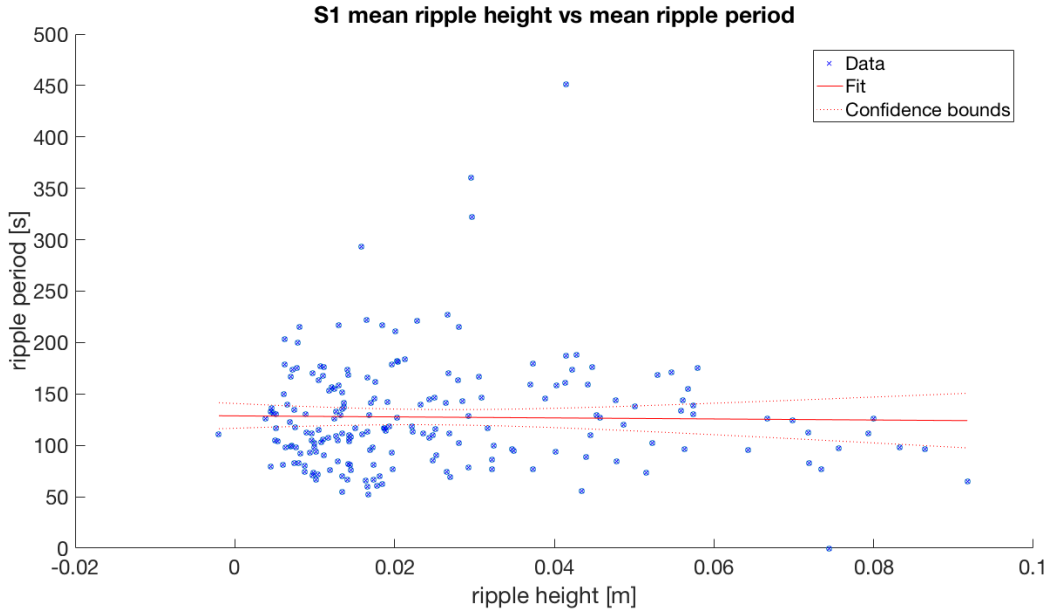

Figure 29 Scatter plot of mean ripple height vs mean period for S1. There is no clear correlation between period and amplitude overall. The blue points from the first two tidal cycle have mostly smaller ripple amplitudes and longer periods (so a steeper slope between the two), while the red points from the last two tidal cycles have a shorter period but a larger amplitude. This location experienced lower waters, so more breaking waves, during the last two tides (S2b).

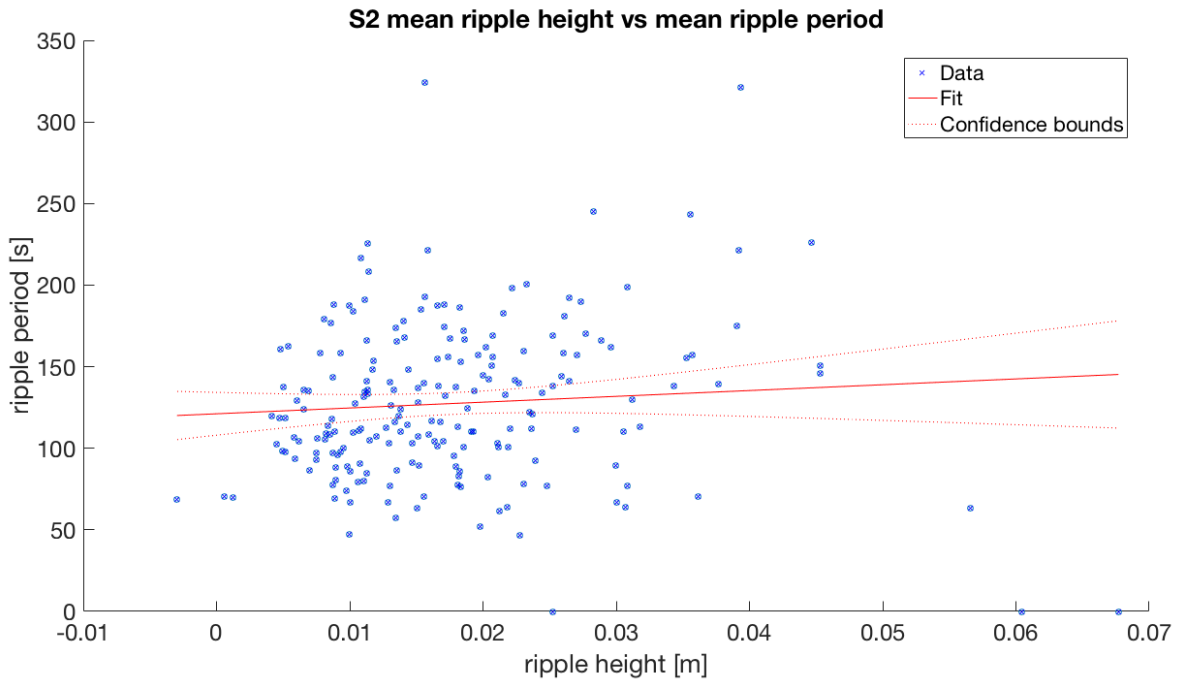

Figure 30 Scatter plot of mean ripple height vs mean period for S2. These points are less scattered than for S1 and generally follow a positive linear trend. This could indicate that this is showing mostly formation time, that larger ripples take longer to form and/or propagate slower. There is no obvious difference between the two times (a and b)

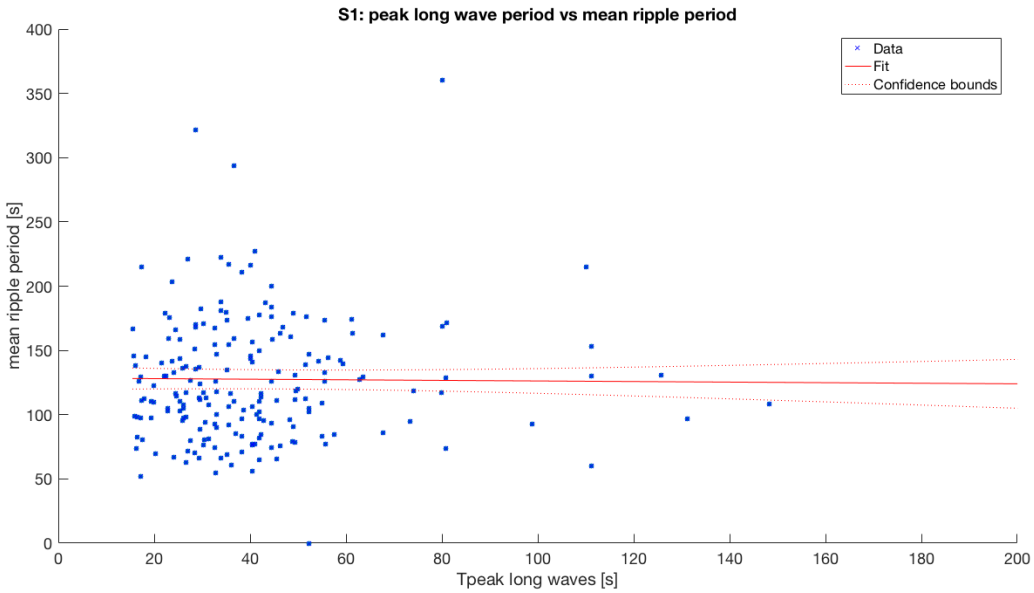

Figure 31 Scatter plot to correlate peak long wave period and mean ripple period. While there is no real correlation, the important thing to note is the order of magnitude of both. The range of the mean ripple periods is twice that of the peak wave periods. The cross correlation shown in the appendix (figure A) does show that this is the strongest correlation.

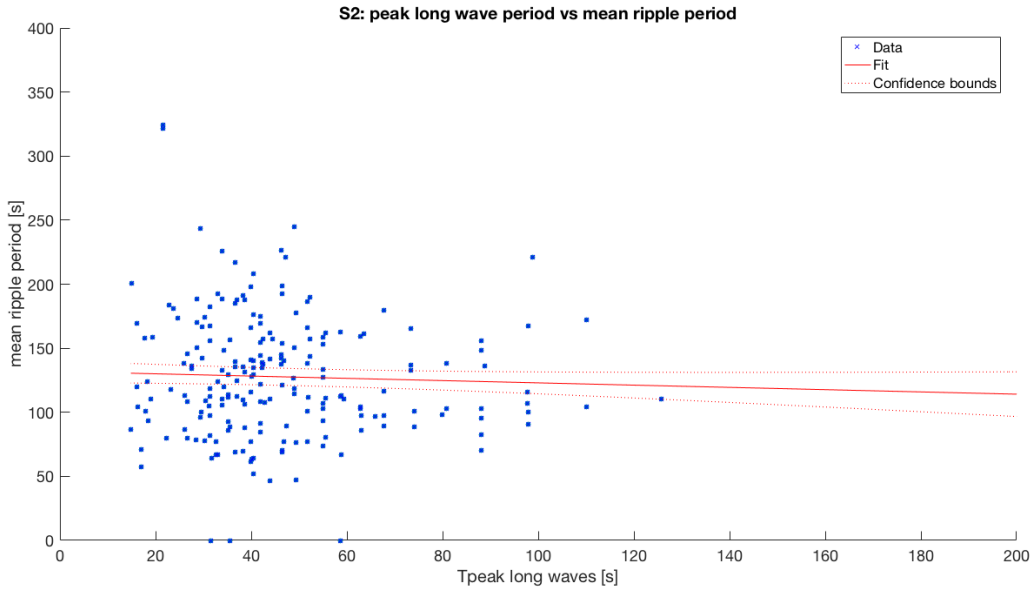

Figure 32 Scatter plot to correlate peak long wave period and mean ripple period. While there is no real correlation, the important thing to note is the order of magnitude of both. The range of the mean ripple periods is twice that of the peak wave periods.

Gamma, the wave height over the water depth, can be used as a way to normalize the wave height by the depth. It is normally used as a breaker index: the wave breaks when its height is a certain fraction of the total depth. Usually this breaker index is defined using the maximum wave height, and a gamma value of 0.88. However, for the significant wave height this value can be defined at about a half, and values of 0.4 to 0.5 indicate breaking waves. (Bosboom and Stive 2015).

$$\gamma = \frac{H}{h}$$

In the scatter plot for the gamma and ripple height from S1 (Figure 33), it can be seen that there is a positive linear trend between gamma and the ripple height during high tide and a negative at low tide for S1. S2 shows a positive linear trend for both, but with a low R^2 value. During the low tide there are more breaking waves, which could be responsible for the higher shear stresses (bottom velocities) and subsequent shortening of the ripples. During high tide, deeper waters, the ripple height increases with gamma. The maximum ripple heights occur for low values of gamma during low tide. For both low and high tide at S2 there is not a big increase or decrease of ripple height with gamma. This could be due to the presence of stronger currents. What both sensors do show is a positive linear trend for the ripple height and gamma at deeper water.

One major component that is missing from this data set is any information on the local current. In lieu of this, assumptions are made regarding the ambient current. Wengrove et al (2018) classifies flow regime by using a fraction of wave energy to combined energy of waves and currents. Their findings over one tidal cycle show that currents are stronger under the higher water depth, and the ratio of energy becomes smaller (more dominated by currents). So it is assumed that currents are generally more dominant in deeper water than shallower water. This is also matching with the theory mentioned earlier from Bosboom and Stive (2015).

Wengrove (2018) also finds larger ripples at the onshore sensor and smaller at the offshore, so the data found here is consistent. This could be damping of the ripple heights due to stronger currents in deeper water. The weaker relation between gamma and ripple height could also be due to this interaction with the current, which changes which type of current is dominant.

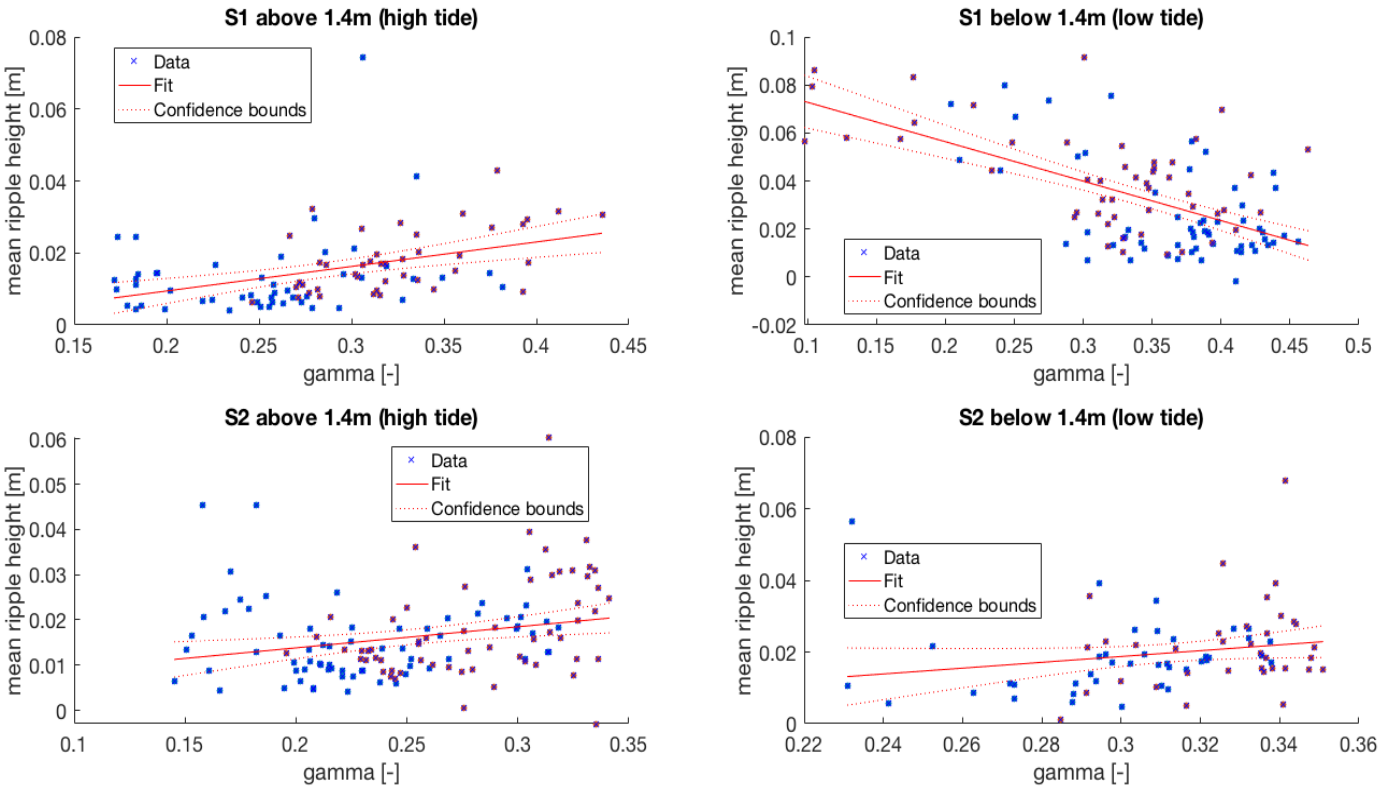

Figure 33 Plots for gamma vs mean ripple height for both sensors split by high and low tide. High tide is defined as all water depths above 1.4m which is the mean of the median values for both sensors, and low tide all water depths below 1.4m. It can be seen that the onshore sensor (S1) has a much stronger correlation. The R^2 value for S1 high tide is .15, and for low tide .35. For S2 these values are .06 for high tide and .03 for low tide, indicating a much weaker correlation.

Initially it was found that a bin of 8 minutes was large enough to include at least one full ripple (two troughs, one peak). The data analysis was done for bins of 8 minutes, and it was found using the function xcorr in MatLab that the shift between parameters to maximize the correlation was always around 1-2 bins. When the bin was extended to 15 minutes, this shift disappeared and parameters became correlated the strongest around a zero shift. This is in agreement with Farari and Foti (2002) who determined 15 minutes for individual ripples to reach equilibrium, as well as the plots from Davis et al (2004) which show the bed adjusts to the new conditions in 15-20 minutes, and results from Lacy et al (2007) who also found it took around 15 minutes to reach an equilibrium. What this means is that the bed adjusts to the wave conditions within 15 minutes. Though it is not possible to tell from this data if the bed has

actually reached equilibrium, for which a wavelength would be needed to calculate steepness, it seems very likely given the correlations that the bed adjusts to the hydrodynamic conditions in about 15 minutes.

5. Discussion

The onshore sensor, S1, showed stronger correlations between variables (eg. wave height and ripple height, skewness and ripple height) for the above scatter plots. This is based on the R^2 values of the linear fits. Additionally, this location had larger ripples than at S2; this is in agreement with results from Wengrove et al (2018), who had sensors in similar locations. Wengrove et al (2018) also found stronger currents at the S2 location than at the S1 location, which could be a possible explanation for the weaker correlations and smaller ripples. This would mean that S1 is located in a more wave-dominated environment where the correlations are stronger. S2 is in an environment where the current is more dominant, causing the ripple amplitudes to be dampened and the correlations to be weakened.

For the S1 location, the reaction time is within 15 minutes. The reaction time is the time it takes for the bed to react, by ripples growing or flattening, to the wave conditions. This is because for a bin size of 15 minutes, there is a strong correlation between ripple height and wave height (and skewness) with a zero time shift. The S2 location showed overall weaker correlations, and the cross correlation analysis did not show that a time shift would improve these. This means that the signal of the bed and the signal of the waves are following each other within 15 minutes. Thus the reaction time of the bed is around 15 minutes. This is also in agreement with other lab research which has looked at how the bed reacts to changing conditions (Faraci and Foti 2002, Davis et al 2004, Lacy et al 2007).

Comparison of the ripple parameters to other papers proved difficult, as most of the papers define ripples by a steepness which includes both ripple height and wavelength, and this study lacked wavelength data. However, this does not mean that the set-up of the sensor for this experiment is completely invalid. Gallagher (1998) used a similar set up of downward facing echo sounders on poles in the near shore, and with smaller spacing between the poles was able to observe propagation speed and wavelength of their megaripples. For future field work with the echo sounders this set up could provide more information on the wavelength of ripples and make comparison with other papers easier.

For the analysis of the bed data that was gathered in this experiment, a band pass filter worked well. This is the same technique used by Davis et al (2004), except they chose the limits of the filter based on the wavelengths of the ripples whereas in this experiment the limits were based on the frequencies of the longwaves. The technique could be refined but overall proved to be a good filter for this type of data.

The evolution of ripples presented in Grant and Madsen (1982) – where ripples form under less energetic conditions, are then flattened under more energetic conditions, and potentially completely flattened out in sheet flow if the conditions exceed the threshold – could be used

to look at a tidally driven sediment transport cycle. Since generally larger ripples occur during low tide, and by high tide they are smaller, if the threshold for sheet flow is exceeded during the transition from low to high tide there could be peaks in sediment transport. Whether or not there is a variation in sediment transport volume in the nearshore during the tidal cycle is an interesting question for future research.

6. Conclusion

The following questions were asked in the introduction:

- What are the amplitudes and time scales of sand ripples?
- Do these change in response to changes in wave parameters?
- What are the general patterns in ripple and wave characteristic? Are there similarities between the two? If so, are there time lags?
- Can wave data be used to predict ripple parameters, height, or time?

These were answered using data collected at the sand motor in the Netherlands using echo sounders and pressure sensors collocated in two locations in the near shore. The data from the waves was analyzed using the zero crossing method and a spectral analysis to find the peak period (where the most energy is). The bed data was filtered using a band pass filter to focus on ripples which had periods on the order of magnitude and longer than those of the long waves. Ripples were defined using a similar technique to the zero crossing method, where one ripple started in the trough and ended in the following trough with a peak in between.

The amplitude and time scales (periods) of ripples found with the peak-trough analysis were around .05-.1 meters and 100-300 seconds, respectively. The most onshore sensor, S1, showed overall larger ripple heights than S2. For both sensors the periods of the ripples were similar. The bed signal was filtered by frequency, so all measured ripple periods are expected to lie between 100 and 1000 seconds. For S1, the mode within this range occurred around 110-150 seconds. For S2 the mode was the same. Most of the ripples were small, with amplitudes around .02 - .05 meters. In general, the largest ripples can be found in shallower waters with waves around .1 m. Smaller ripples occur throughout, but are dominant in deep water or under small wave conditions.

The mean period of the ripples is on the same order of magnitude as the long wave period, though they are not correlated. There do exist ripples or bedforms with larger periods, more than 1000 seconds, which were filtered out for this study. Further studies using both downward facing and side scanning sonars, or closely spaced downward facing sonars, could be used to ascertain which part of the ripple period is propagation and which is formation.

Because no data on currents is available, exact bottom velocity, ratio of current to wave energy, and angle between the two vectors cannot be determined. However, from relative estimates of the long shore current it is likely that the ratio of current to wave energy is higher

for S2 and this explains the overall smaller ripples and the larger wave height needed to reach a maximum ripple amplitude.

Directly from the results of this paper, the answer to the last question is: no. No equations were written for ripples parameters based on the wave parameters. The ripple period did not have any strong correlations; this is due to the propagation speed (or migration rate) and the formation speed being inseparable in the ripple period data. Future studies should take into consideration when measuring ripples that the wavelength is an important parameter for characterizing ripples.

Ripple amplitude was correlated with both the skewness and amplitude of the waves, and there also appeared to be a relationship between ripple amplitude and gamma for S1. With more information on currents, such as when and by how much they affect the ripple behavior, it is possible to predict ripple heights from wave conditions. This work is a small step towards accurately modeling bed texture and behavior based on wave information.

7. Bibliography

Battjes, J. A. (1988). Surf-zone dynamics. Annual Review of Fluid Mechanics, 20(1), 257-291.

Bosboom, Judith, Marcel Stive. Coastal Dynamics 1: lecture notes CIE4305. Delft Academic Press. 2015.

Carstens, M. R., Neilson, F. M., & Altinbilek, H. D. (1969). *Bed forms generated in the laboratory under an oscillatory flow: analytical and experimental study* (No. 28). US Army Corps of Engineers, Coastal Engineering Research Center.

Davis, J. P., Walker, D. J., Townsend, M., & Young, I. R. (2004). Wave-formed sediment ripples: Transient analysis of ripple spectral development. *Journal of Geophysical Research: Oceans*, *109*(C7).

Dingler, J. R., Inman, D. L. (1977). Wave-formed ripples in nearshore sands. In Coastal Engineer-ing 1976 (pp. 2109-2126).

Faraci, C., & Foti, E. (2002). Geometry, migration and evolution of small-scale bedforms generated by regular and irregular waves. *Coastal Engineering*, *47*(1), 35-52.

Gallagher, E. L., Elgar, S., & Thornton, E. B. (1998). Megaripple migration in a natural surf zone. *Nature*, *394*(6689), 165-168.

Grant, W. D., & Madsen, O. S. (1982). Movable bed roughness in unsteady oscillatory flow. *Journal of Geophysical Research: Oceans*, *87*(C1), 469-481.

Jain, S. C., & Kennedy, J. F. (1974). The spectral evolution of sedimentary bed forms. *Journal of Fluid Mechanics*, *63*(2), 301-314.

Lacy, J. R., Rubin, D. M., Ikeda, H., Mokudai, K., Hanes, D. M. (2007). Bed forms created by simulated waves and currents in a large flume. Journal of Geophysical Research: Oceans, 112(C10).

Longuet-Higgins, M. S. (1981). Oscillating flow over steep sand ripples. Journal of Fluid Mechanics, 107, 1-35.

Marsh, S. W., Vincent, C. E., & Osborne, P. D. (1999). Bedforms in a laboratory wave flume: an evaluation of predictive models for bedform wavelengths. *Journal of coastal research*, 624-634.

Nielsen, P. (1981). Dynamics and geometry of wave generated ripples. Journal of Geophysical Research: Oceans, 86(C7), 6467-6472.

O'Donoghue, T., Clubb, G. S. (2001). Sand ripples generated by regular oscillatory flow. Coastal Engineering, 44(2), 101-115.

Ribberink, J. S., Al Salem, A. A. (1994). Sediment transport in oscillatory boundary layers in cases of rippled beds and sheet flow. Journal of Geophysical Research: Oceans, 99(C6), 12707-12727.

Roelvink, J. A., Stive, M. J. F. (1989). Bar generating cross shore flow mechanisms on a beach. Journal of Geophysical Research: Oceans, 94(C4), 4785-4800.

Wengrove, M. (2018). Bedform Geometry and Bedload Sediment Flux in Coastal Wave, Current, and Combined Wave-Current Flows.

Wengrove, M. E., Foster, D. L., Lippmann, T. C., de Schipper, M. A., Calantoni, J. (2018). Ob-servations of Time Dependent Bedform Transformation in Combined Wave Current Flows. Journal of Geophysical Research: Oceans, 123(10), 7581-7598.

Wengrove, M. E., Henriquez, M., De Schipper, M. A., Holman, R., Stive, M. J. F. (2013). Monitoring morphology of the sand engine leeside using Argus' cBathy. In Coastal

Dynamics 2013: 7th Interna-tional Conference on Coastal Dynamics, Arcachon, France, 24-28 June 2013. Bordeaux University.

Wiberg, P. L., & Harris, C. K. (1994). Ripple geometry in wave-dominated environments. *Journal of Geophysical Research: Oceans*, *99*(C1), 775-789.

Appendix A: filters and time lag

A.1. only using the moving mean

Only using the moving mean underestimated ripple properties due to it recognizing mostly noise as ripples and thereby overlooking the actual ripple. An example of how the script recognizes ripples is shown in figure 3.3, and the full time series of both sensors in figures 4.3 and 4.4.

Ripple periods are the same order of magnitude as the long wave periods. To see if these are related a cross correlation is made, presented in figure 8.4. This shows peaks between -1 and +1. The positive lags indicate the wave period is leading the ripple period. The negative correlation in that case does not make sense, but there is a second peak at zero which is very close in value to the one at -1. Over all four datasets then, the lag is between zero and 8 minutes. This can be real, however since both datasets are fairly noisy this is not a very reliable measure of lag time between the two. The same is done for the wave height in figure 8.3. Since the energy in the wave spectrum is linearly related to the wave height squared (variance). The comparison of the two is analogous to comparing the energy in each block of the signal.

A.2. Lowpass filtered data analysis

Didnt make any difference to the signal compared to only taking the mean (see above section). This could be due to badly parameterized filter, but the band pass highlighted the frequencies of interest so its fine. Perfecting the low pass filter would mean being able to look at the more low frequency oscillations in the bed.

A.3. Matching the frequencies of data

Matching the frequencies of the data partially works. The interp() fuction in matlab does linearly inter-polate, however because the frequency of the bed data is not an even number it isn't perfect. This could be easily solved by writing a new script to interpolate, but this didn't really fit the analysis done for this paper since the mean/peak values over steps in time would be taken anyway. Would be appropriate for small time scale analysis, to see how waves instantaneously effect the bottom.

Appendix B: Flowchart of scripts and functions used to process data